LU TP 15-nn
June 2015

Flavour-changing neutral currents in top quark decays to Higgs bosons in a two-Higgs-doublet model

Leo Zethraeus

Department of Astronomy and Theoretical Physics, Lund University

Bachelor thesis supervised by Johan Rathsman

Abstract

In this thesis top quark decays to a charm quark and a (CP even) Higgs boson (ϕ) are investigated in a general two-Higgs-doublet model (2HDM) allowing flavour-changing neutral currents. The theory behind 2HDMs is introduced and the specific choice of 2HDM is put to test under theoretical constraints that require the potential in the Lagrangian density of the model to satisfy vacuum stability, tree-level unitarity and perturbativity. The parameter space of the specific 2HDM is also restricted by recent data from the LHC on the signal strengths of the discovered Higgs boson in the $\gamma\gamma$ and ZZ decay channels. In addition, constraints from a recent measurement of $Br(t \to c\phi)$ are taken into account. This puts restrictions on the values of the off-diagonal Yukawa coupling ρ_{ct} appearing in the $t \to c\phi$ decay. It is found that the commonly used Cheng-Sher ansatz regarding the order of magnitude of this flavour-changing neutral coupling is not severely constrained by the measurement.

Populärvetenskaplig beskrivning

Först lite terminologi: Standardmodellen är en kvantfältteori. Sådana beskriver störningar i fält och dessa kallas för partiklar. Tänk dig svallvågorna som följer på ytan i ett badkar vari en sten släppts, fast i tre dimensioner istället för två, det är ett fält. Varje elementär partikel är en störning i ett sådant tillhörande fält (eller "kvantum" varav namnet kvantfält). Fälten kommer i två sorter: fermionska och bosonska. De förstnämnda fälten beskriver all materia vi känner till, samt lite till som kan skapas i acceleratorer men som inte är något vi stöter på till vardags. Bosonfält beskriver hur fermionfält interagerar med varandra, hur störningar i ett fält kan orsaka störningar i ett annat. Ett bekant bosonfält är det elektromagnetiska, som även är känt som ljus. Störningar i detta fält kallas för fotoner.

Higgsfältet framlades som ett förslag på 60-talet för att lösa problemet med varför vissa (både fermion och boson) partiklar har massa. Cirka 50 år senare hittades en Higgsboson (störning i det bosonska Higgsfältet) med rätt egenskaper såsom förutsagda av Standardmodellen. Teorin beskriver massans ursprung på ett liknande sätt som andra interaktioner och sätter dem nästan på jämn fot. Olika fält interagerar med Higgsfältet olika mycket och detta gör att partiklarna får olika massa. De blir "tröga", som fysiker säger om partiklar med massa, av att färdas genom Higgssoppan. Att ha massa är nämligen ett annat sätt att säga "att inte färdas i ljusets hastighet".

Fysiker tycker att enkelt är snyggt (och praktiskt), därför har man i Standardmodellen antagit att det bara finns ett Higgsfält som ger upphov till alla massor. Det finns dock stora anledningar att låta fler Higgsfält sköta jobbet. I den enklaste utvidgningen av teorin inför man istället två Higgsdubletter som trots namnet introducerar fem nya partiklar i teorin. Många vidare teorier som kan förklara varför laddning är kvantiserad och mörk materia (med trevliga ord som supersymmetri och storförenade teorier) kräver minst detta för att fungera.

I denna uppsats har jag undersökt en konsekvens av detta "första steg mot en allmännare teori". En ny teori ska helst förklara allt som Standardmodellen förklarar och lite till, så att man kan särskilja dem med experiment. En sådan skiljelinje visar sig vid sönderfall av en toppkvark till en charmkvark[1] och en (valfri)[2] Higgsboson. Detta sönderfall sker nästan aldrig enligt Standardmodellen men kan göra det i två-Higgs-dublett modeller.

Jag har undersökt hur vanligt förekommande detta sönderfall får och kan vara, enligt teoretiska och experimentella begränsningar. Sönderfallet är speciellt för just en viss sorts två-Higgs-dublett modell (kallad 2HDM-III), i alla andra varianter är det väldigt sällsynt. Om det går att hitta en signal för detta sönderfall, så skulle alltså alla andra sorters två-Higgs-dublett modeller och de teorier som bygger vidare på dessa, visa sig vara felaktiga. Många flugor i en smäll, med andra ord.

[1] Ytterligare några fermioner: De kommer i flera smaker. Smak är faktiskt den tekniska termen. Ett topp- till charm sönderfall kallas för en smakändrande (neutral) ström.

[2] Men elektriskt neutral, om man ska vara petig.

Contents

Abbreviations

2HDM
Two-Higgs-Doublet Model

FCNC
Flavor-Changing Neutral Current

SM
Standard Model

VEV
Vacuum Expectation Value

2HDMC
Two-Higgs-Doublet Model Calculator

LHC
Large Hadron Collider

CP
Charge-Parity

1 Introduction

The Standard Model has been successful at describing most interactions between fundamental particles, and in 2012 the LHC group announced the discovery of the long sought-for Higgs boson [1]. However, this is not the end of particle physics. Many questions are still left unanswered, for example; why is charge quantized? Why is gravitation so weak? What is dark matter?

The scalar boson found at LHC is consistent with the Standard Model Higgs theory by all the data obtained so far. It is of great interest to further study its properties, as any deviations from the Standard Model can indicate which extended theories that are compatible with observations, to know where to proceed next.

The Standard Model is an effective theory meaning it claims only to explain physics up to a certain energy scale. Beyond this, new physics must necessarily arise. A new good effective theory must incorporate the Standard Model at the relevant energy scale, but also predict new phenomena. One approach to this is to extend the minimal Brout-Englert-Higgs mechanism used in the Standard Model to contain two complex doublets, resulting in five physical particles and three Goldstone bosons. Models that are based on this assumption are called two-Higgs-doublet models, 2HDMs for short. 2HDMs are interesting because for a minimum added complexity, a lot of interesting (and experimentally testable) phenomena, that doesn't occur in the Standard Model, are allowed to occur in 2HDMs. One of these phenomena is the occurrence of flavour-changing neutral currents (FCNCs) at tree-level, which is forbidden in the Standard Model. These FCNCs provide a good test to compare different models beyond the Standard Model.

There are stringent limits on FCNCs from meson oscillations [2] which puts strong restrictions on the models in which they occur naturally at tree-level. The rarity of FCNCs has led physicists [3] to formulate versions of 2HDMs[3] that are naturally free of FCNCs at tree-level. This can be done by imposing a Z_2 symmetry on the Higgs couplings to fermions.

There are many variants of 2HDMs that are free of FCNCs at tree-level, each imposing different Z_2 symmetries and thereby removing some degrees of freedom from the Lagrangian. The most popular of these is called Type II. As Type II is favoured in extended theories requiring supersymmetry, much work has been done on the implications of this model and restrictions based on current experimental data. If no assumption of extra symmetry is made[4], one obtains 14 degrees of freedom in the potential and 27 degrees of freedom in the Yukawa sector, among which some lead to FCNCs at tree-level.

Three of the new particles introduced in 2HDMs are neutral scalar bosons h, H and A that can mediate FCNCs.[5] It is assumed that one of the neutral scalars is the particle found at LHC, and the other two have unknown masses. The particle found at LHC is one of the two scalars h or H. Two cases arise: either the particle found is the heavier of the two (in this thesis called either case $m_H = 125\,\mathrm{GeV}/c^2$ or the heavy found Higgs case), or

[3]Type I, II, Type - LS and Type - Flipped

[4]In this thesis referred to as Type III

[5]Two are spin-zero scalars (h, H) and one is a pseudoscalar (A) in fermion interactions (CP-odd)

it is the lighter one (case $m_h = 125\,\mathrm{GeV}/c^2$ or the light found Higgs case).[6] The remaining scalar bosons in 2HDMs are electrically charged. The properties of these charged bosons will not be treated in this thesis.

The most significant difference between 2HDM-III and the Standard Model is the occurrence of FCNCs, and one of these FCNCs comes from top quark decay to a charm quark and a Higgs boson at tree-level. The Higgs boson can be any of the three neutral scalars and all cases can in general contribute to the branching ratio. This decay occurs in the Standard Model but only through loops and is forbidden at tree-level, making the branching ratio too small to ever be observed.

In the 2HDM Type III, the branching ratio could be within detectable limits depending on the values of an undetermined Yukawa coupling and a parameter-space angle. A recent measurement have put an upper limit to $Br(t \to c\phi)$ ($\phi = h,\ H,\ A$) [4], and this restricts the value of the coupling. Under the commonly used Cheng-Cher ansatz [5], the order of magnitude of the Yukawa couplings is estimated so as to not give too large FCNCs and still be natural. If the Yukawa coupling related to $t \to c\phi$ is required by the measurement to be many orders of magnitude larger or smaller than unity, the 2HDM - III may face problems with fine-tuning.

The parameter-space angle relates the found Higgs boson h (H), to the undiscovered Higgs boson H (h). Therefore, experimental restrictions on signal strengths through processes measured at the LHC restricts also the allowed parameters in a 2HDM. Explicitly, the branching ratio $Br(t \to c\phi)$ depends on four undetermined parameters (the Yukawa coupling, the parameter-space angle and two unknown masses of the neutral Higgs bosons). But theoretical considerations such as vacuum stability, tree-level unitarity and perturbativity introduces implicit relations between all free parameters in the theory, and these relations must be satisfied in every type of 2HDM.

The purpose of this thesis is to investigate the $t \to c\phi$ decay under theoretical constraints and experimental restrictions on the parameter space of a 2HDM - III. The outline is as follows: In Section 2 the Standard Model and the minimal Brout-Englert-Higgs mechanism is reviewed. The theory behind two-Higgs-doublet models and the theoretical constraints on the parameters of the potential is introduced in Section 3. In Section 4 the Yukawa Lagrangian is expressed in different bases and the relations between different 2HDMs with Z_2 symmetries is explained. Towards the end of Section 4, the general 2HDM-III that allows FCNCs is introduced and restricted by some assumptions. The branching ratio $\Gamma(t \to c\phi)$ is given in Section 4.4 (derived in Appendix A). In Section 5 the experimental restrictions from measurements of the properties of the discovered Higgs boson in the $\phi \to \gamma\gamma$ and $\phi \to ZZ$ decay channels are discussed and all the results are presented and discussed in Section 6. The conclusions drawn from the results are summarized in Section 7 along with an outlook for further investigations.

[6] By common convention, H always denotes the heavier of the two neutral scalar fields (found or not) and h the lighter.

2 Symmetries in the Standard Model

This section will describe how the minimal Brout-Englert-Higgs mechanism used in the Standard Model works. Those who are familiar with it may skip to Section 3. The reasoning throughout this section is heavily inspired by [6] and most equations in this section are obtained from Chapter 8 in [6].

The Standard Model Lagrangian $\mathcal{L}_{SM} = T - V$ describes all interactions between particles observed. It contains kinetic terms T and interaction terms in the potential V. The Lagrangian of the Standard Model is made invariant under operations of SU(3) x SU(2) x U(1) which in turn gives rise to gauge bosons and interaction terms between gauge bosons and fermions. This is all seen explicitly by adding new terms in the covariant derivative in order to keep $\mathcal{L}$ invariant under rotations in the different spaces. All fermion interactions[7] in the first generation are described by [6]:

$$\mathcal{L}_{\text{fermion,G1}} = \sum_{\text{f=L, } e_R, \text{ } (\nu_R), \text{ } Q_L, \text{ } u_R, \text{ } d_R} \overline{f} i\gamma^\mu \mathcal{D}_\mu f, \tag{2.1}$$

where the left-handed leptons and quarks are put in SU(2)-doublets $L = (\nu_{eL}, e_L)^T$,[8] $Q_L = (u, d)^T$ and the right-handed terms are SU(2)-singlets. The other generations can be included by simply adding terms like $\mathcal{L}_{\text{fermion,G1}}$ but with $e \to \mu, \tau$, $\nu_e \to \nu_\mu, \nu_\tau$, $u \to c, t$ and $d \to s, b$ for both the left-handed and right-handed terms. A general U(1) symmetry means that the theory makes the same predictions (which requires that $\mathcal{L}$ keeps the same form) if f is changed to f' by the transformation

$$f \to f'_{\text{U(1)}} = e^{i\theta(x)} f \qquad \text{U(1)}. \tag{2.2}$$

This is called a local U(1) symmetry since the phase $\theta(x)$ is allowed to depend on position. $\mathcal{L}_{\text{SM}}$ is also invariant under rotations in SU(2) and SU(3) space. This means that the transformations:

$$f \to f'_{\text{SU(2)}} = e^{i\epsilon^i(x)\cdot\tau^i} f \qquad \text{SU(2)}, \tag{2.3}$$

where the τ_i ($i = 1,\ 2,\ 3$) are the Pauli matrices and for the quark SU(3) terms (with the Gell-Mann matrices λ_a , $a = 1,\ ...,\ 8$):

$$f \to f'_{\text{SU(3)}} = e^{i\alpha^a(x)\cdot\lambda^a} f \qquad \text{SU(3)}, \tag{2.4}$$

leaves $\mathcal{L}$ unchanged.

The full covariant derivative that keeps $\mathcal{L}$ invariant under SU(3) x SU(2) x U(1) is:

$$\mathcal{D}_\mu = \partial_\mu - ig_1 \frac{Y}{2} B_\mu - ig_2 \frac{\tau^i}{2} W^i_\mu - ig_3 \frac{\lambda^a}{2} G^a_\mu. \tag{2.5}$$

[7] Assuming they are massless.

[8] The notation $(\nu_{eL}, e_L)^T = \binom{\nu_{eL}}{e_L}$ is used for spatial convenience.

Where g_i are the gauge couplings, Y is the hypercharge, B_μ is the gauge field required to keep $\mathcal{L}$ invariant under U(1), W_μ^i for SU(2) and G_μ^a for SU(3).

Equation (2.1) is essentially the Dirac-equation for massless particles, with additional gauge terms in the covariant derivative $\mathcal{D}_\mu$ in order to keep $\mathcal{L}$ invariant under the above mentioned symmetries. One important thing should be noted: equation (2.1) is assuming all fermions to be massless, but they are not. Adding a mass term m to Eq. (2.1), $\mathcal{D}_\mu \rightarrow (\mathcal{D}_\mu - m)$ would break the SU(2) symmetry explicitly. The same problem occurs for the gauge particles, mass terms of the required dimension $m^2 W_\mu^+ W^{\mu-}$ cannot simply be added to the Lagrangian without breaking the SU(2) symmetry.

2.1 The Minimal Brout-Englert-Higgs Mechanism

There's a neat way to give mass to the particles, developed by Brout, Englert and Higgs in the 60's [7] [8], that breaks the SU(2) symmetry of $\mathcal{L}$ only at one point, the ground state (or vacuum) of the potential.

An additional spin-zero field is added to the theory in the form of a SU(2) doublet:

$$\Phi = \begin{pmatrix} \Phi^+ \\ \Phi^0 \end{pmatrix} = \begin{pmatrix} \phi_1 + i\phi_2 \\ \phi_3 + i\phi_4 \end{pmatrix}, \tag{2.6}$$

where Φ^+ and Φ^0 are complex fields. The Lagrangian for the spinless doublet is:

$$(\mathcal{D}_\mu \Phi)^\dagger \mathcal{D}^\mu \Phi - \mu^2 \Phi^\dagger \Phi - \lambda (\Phi^\dagger \Phi)^2, \tag{2.7}$$

where $\mathcal{D}^\mu$ is the covariant derivative including the Electro-Weak SU(2) x U(1) gauge fields and μ^2 and λ are free parameters. Focusing on the potential of the field:

$$V = \mu^2 \Phi^\dagger \Phi + \lambda (\Phi^\dagger \Phi)^2 \tag{2.8}$$

This 'Mexican hat' potential has a minimum at $\Phi^\dagger \Phi = 0$ if $\mu^2 > 0$ and at $\Phi^\dagger \Phi = \frac{-\mu^2}{2\lambda} \equiv \frac{v^2}{2}$ if $\mu^2 < 0$. Since there are four fields in $\Phi^\dagger \Phi = \phi_1^2 + \phi_2^2 + \phi_3^2 + \phi_4^2$. The minimum can be reached in a non-trivial (four-dimensional Mexican hat) way:

$$\Phi^\dagger \Phi = \phi_1^2 + \phi_2^2 + \phi_3^2 + \phi_4^2 = \frac{v^2}{2}.$$

Picking, quite arbitrarily, the point $\phi_3 = v$, $\phi_1 = \phi_2 = \phi_4 = 0$ the SU(2) doublet field can be expanded around this point (the vacuum),

$$\Phi = \frac{1}{\sqrt{2}} \begin{pmatrix} 0 \\ v + h(x) \end{pmatrix}. \tag{2.9}$$

Put into the potential part of (2.8) yields a mass term for the field $h(x)$:

$$-\frac{1}{2}(2\lambda v^2) h^2(x) \equiv -\frac{1}{2} m_h^2 h^2(x).$$

Writing the relevant part of the first term in (2.7) with U(1) and SU(2) terms from the covariant derivative explicitly (the SU(3) term is omitted since Φ is a SU(2) doublet and a SU(3) term acting on it gives zero by definition and the normal derivative ∂_μ is not interesting for the purpose of generating mass):

$$\Phi^\dagger\Big(ig_1\frac{Y}{2}B_\mu + ig_2\frac{\vec{\tau}}{2}\cdot\vec{W}_\mu\Big)^\dagger\Big(ig_1\frac{Y}{2}B^\mu + ig_2\frac{\vec{\tau}}{2}\cdot\vec{W}^\mu\Big)\Phi. \tag{2.10}$$

Evaluating this gives

$$\frac{1}{8}v^2g_2^2\Big((W_\mu^1)^2 + (W_\mu^2)^2\Big) + \frac{1}{8}v^2(g_1B_\mu - g_2W_\mu^3)^2.$$

The linear combination of B_μ and W_μ^3 appearing in the second term is proportional to the physical particle denoted by Z_μ, $Z_\mu \propto (g_1B_\mu - g_2W_\mu^3)$ and the first term in brackets is $2W_\mu^+W^{-\mu}$. So,

$$\Big(\frac{1}{2}vg_2\Big)^2W_\mu^+W^{-\mu} + \frac{1}{2}\Big(\frac{1}{2}v\sqrt{g_1^2+g_2^2}\Big)^2Z_\mu Z^\mu \equiv m_W^2W_\mu^+W^{-\mu} + \frac{1}{2}m_Z^2Z_\mu Z^\mu.$$

And thus, the gauge vector bosons have acquired mass. Note that there is a factor of 2 difference between the mass terms for a charged gauge boson and a neutral one. Note also that no mass terms of the sort:

$$\frac{1}{2}m_A^2(g_2B_\mu + g_1W_\mu^0) = \frac{1}{2}m_A^2A_\mu A^\mu$$

appears, the photon remains massless.

The fermions (except for the neutrinos) of the first generation can be given mass using a different Lagrangian (which from now on will be denoted $\mathcal{L}_{\text{yukawa}}$):

$$\mathcal{L}_{\text{yukawa}} = g_e\overline{L}\Phi e_R^- + g_d\overline{Q}_L\Phi d_R + g_u\overline{Q}_L(-i\tau_2\Phi^*)u_R + \text{h.c.} \tag{2.11}$$

When expanded around the vacuum of (2.9) this expression becomes:

$$\mathcal{L}_{\text{yukawa}} = \frac{g_ev}{\sqrt{2}}\overline{e}e + \frac{g_dv}{\sqrt{2}}\overline{d}d + \frac{g_uv}{\sqrt{2}}\overline{u}u + \frac{g_e}{\sqrt{2}}\overline{e}eh + \frac{g_d}{\sqrt{2}}\overline{d}dh + \frac{g_u}{\sqrt{2}}\overline{u}uh. \tag{2.12}$$

The first three terms have the right dimensions to be interpreted as mass terms $m_f = \frac{g_fv}{\sqrt{2}}$ and the last three terms represent interactions with a field h.

The same Lagrangian (with obvious substitutions) can generate mass for the other generations as well.

3 2HDM

As the name suggest, in a two-Higgs-doublet model two doublets of the form (2.6) are introduced [9]. This gives rise to 5 physical fields and three Goldstone fields that turn into the longitudinal polarisations of the $W^{\pm}$ and Z. In addition, many new parameters are introduced that make the model slightly more intricate than the minimal Brout-Englert-Higgs mechanism in the Standard Model, but many new interesting phenomena can occur. The basic idea is the same; a non-zero vacuum expectation value breaks the SU(2) x U(1) symmetry and mass terms arise. The theory is described in this and the following section.

3.1 Generic Potential

With two complex scalar SU(2) doublets $\Phi_{1,2}$, a gauge-invariant and renormalizable potential can be written [10]:

$$\begin{aligned} V \; &= m_{11}^2 \Phi_1^\dagger \Phi_1 + m_{22}^2 \Phi_2^\dagger \Phi_2 - \left[m_{12}^2 \Phi_1^\dagger \Phi_2 + \text{h.c.} \right] \\ &+ \frac{1}{2}\lambda_1 \Big(\Phi_1^\dagger \Phi_1 \Big)^2 + \frac{1}{2}\lambda_2 \Big(\Phi_2^\dagger \Phi_2 \Big)^2 + \frac{1}{2}\lambda_3 \Big(\Phi_1^\dagger \Phi_1 \Big) \Big(\Phi_2^\dagger \Phi_2 \Big) + \frac{1}{2}\lambda_4 \Big(\Phi_1^\dagger \Phi_2 \Big) \Big(\Phi_2^\dagger \Phi_1 \Big) \\ &+ \left\{ \frac{1}{2}\lambda_5 \Big(\Phi_1^\dagger \Phi_2 \Big)^2 + \lambda_6 \Big(\Phi_1^\dagger \Phi_1 \Big) \Big(\Phi_1^\dagger \Phi_2 \Big) + \lambda_7 \Big(\Phi_2^\dagger \Phi_2 \Big) \Big(\Phi_1^\dagger \Phi_2 \Big) + \text{h.c.} \right\}. \end{aligned} \tag{3.1}$$

As will be discussed in detail later, the differences between various models of this kind (usually called 2HDM I, II, III) consist of imposing different symmetries that require some of the parameters to vanish. In the most general model, all parameters can have non-zero values and (with CP-violation allowed) the parameters m_{12}^2 and $\lambda_{5,6,7}$ are allowed to be complex. Imposing a Z_2 - symmetry ($\Phi_1 \to \Phi_1$, $\Phi_2 \to -\Phi_2$) require m_{12}^2 and $\lambda_{6,7}$ to be zero. The parameter m_{12}^2 is soft-breaking since the Z_2 symmetry is regained in the high-energy limit (more on this in section 4.1). The two complex SU(2) doublet fields can be written:

$$\Phi_1 = \begin{pmatrix} \phi_1 + i\phi_2 \\ \phi_3 + i\phi_4 \end{pmatrix}, \quad \Phi_2 = \begin{pmatrix} \phi_5 + i\phi_6 \\ \phi_7 + i\phi_8 \end{pmatrix}.$$

A vacuum expectation value (abbr. vev) of the respective doublets that breaks $\mathrm{SU(2)\,x\,U(1)_Y}$ but keeps the $\mathrm{U_{EM}}$ symmetry can be written [10]:

$$\langle \Phi_1 \rangle = \frac{v}{\sqrt{2}} \begin{pmatrix} 0 \\ \cos\beta \end{pmatrix}, \quad \langle \Phi_2 \rangle = \frac{v}{\sqrt{2}} \begin{pmatrix} 0 \\ e^{i\xi} \sin\beta \end{pmatrix} \tag{3.2}$$

where v is the same as in the Standard Model, eq. (2.9). In the rest of this thesis CP-conservation will be assumed which follows by putting $\xi = 0$ and requiring that m_{12}^2 and $\lambda_{5,6,7}$ are real. The angle β has been introduced such that

$$\tan\beta = \frac{\langle \Phi_2 \rangle}{\langle \Phi_1 \rangle}$$

which is true only if CP is conserved. In the following, the notation $s_\beta = \sin\beta$, $c_\beta = \cos\beta$ and $s_{\beta-\alpha} = \sin(\beta-\alpha)$ will be used.

With the generic potential in 3.1 acquiring a vev as in 3.2, some mass terms arise such as:

$$m_A^2 = \frac{m_{12}^2}{\sin\beta\cos\beta} - \frac{v^2}{2}(2\lambda_5 + \lambda_6\cot\beta + \lambda_7\tan\beta), \tag{3.3}$$

and

$$m_{H^\pm}^2 = m_A^2 + \frac{v^2}{2}(\lambda_5 - \lambda_4). \tag{3.4}$$

The other mass terms can be summarised in the following mass matrix M:

$$M^2 = m_A^2 \begin{pmatrix} s_\beta^2 & -s_\beta c_\beta \\ -s_\beta c_\beta & c_\beta^2 \end{pmatrix} + v^2 \begin{pmatrix} \lambda_1 c_\beta^2 + 2\lambda_6 s_\beta c_\beta + \lambda_5 s_\beta^2 & (\lambda_3+\lambda_4)s_\beta c_\beta + \lambda_6 c_\beta^2 + \lambda_7 s_\beta^2 \\ (\lambda_3+\lambda_4)s_\beta c_\beta + \lambda_6 c_\beta^2 + \lambda_7 s_\beta^2 & \lambda_2 s_\beta^2 + 2\lambda_7 s_\beta c_\beta + \lambda_5 c_\beta^2 \end{pmatrix} \tag{3.5}$$

Since the mass matrix contains off-diagonal terms, a rotation by an angle α can be performed to get to the mass eigenstate with eigenvalues m_H^2, m_h^2 :

$$R(\alpha)M^2R^T(\alpha) = \begin{pmatrix} m_H^2 & 0 \\ 0 & m_h^2 \end{pmatrix} \tag{3.6}$$

In terms of the elements of the mass matrix in (3.5), the eigenvalues are:

$$m_{H,h}^2 = \frac{1}{2}\Big[M_{11}^2 + M_{22}^2 \pm \sqrt{(M_{11}^2 - M_{22}^2)^2 + 4(M_{12}^2)^2}\Big] \tag{3.7}$$

These in addition to m_A and $m_{H^\pm}$ are the physical masses in a 2HDM with CP-conservation.

In terms of the fields in the physical mass-eigenstate basis, the original doublets (Φ_1, Φ_2) can be expressed as [10]:

$$\Phi_1 = \frac{1}{\sqrt{2}}\begin{pmatrix} \sqrt{2}(G^+\cos\beta - H^+\sin\beta) \\ v\cos\beta - h\sin\alpha + H\cos\alpha + i(G^0\cos\beta - A\sin\beta) \end{pmatrix}, \tag{3.8}$$

$$\Phi_2 = \frac{1}{\sqrt{2}}\begin{pmatrix} \sqrt{2}(G^+\sin\beta + H^+\cos\beta) \\ v\sin\beta + h\cos\alpha + H\sin\alpha + i(G^0\sin\beta + A\cos\beta) \end{pmatrix}. \tag{3.9}$$

Where $G^\pm$, G^0 are three Goldstone bosons that turn into the longitudinal polarisation states of $W^\pm$ and Z as they propagate and h, H, A and $H^\pm$ are the physical fields with masses as in (3.7), (3.3) and (3.4).

The two-Higgs-doublet model calculator (2HDMC) [10] is a program that can calculate various observables in any (CP-conserving) 2HDM with or without Z_2 symmetries once the free parameters of the specific model are set. The 2HDMC has been updated and used to calculate branching ratios and check the parameter-space of the model under consideration in this thesis.

3.2 Theoretical constraints

In what follows, the theoretical considerations that are used when checking allowed parameters in the model will be described briefly.[9] All of these constraints are implemented in the 2HDMC [10] and can be checked once a given set of parameters (m_h, m_H, m_A, $m_{H^\pm}$, m_{12}^2, $\sin(\beta-\alpha)$, $\tan\beta$ in the physical basis or λ_i's in the generic basis) have been specified. This routine is used when checking the parameter points in Section 6.

3.2.1 Vacuum stability

For the vacuum to be stable the potential in (3.1) needs to be bounded from below. The potential must not reach negative infinity for large values of the fields in any direction in $(\Phi_1^\dagger\Phi_1,\ \Phi_2^\dagger\Phi_2)$-space. This is only true for some sets of values of the λ_i's in the generic potential (3.1). The constraints on the λ_i's due to vacuum stability are summarized as follows:

$$\lambda_1,\ \lambda_2 > 0 \quad , \quad \lambda_3 > -\sqrt{\lambda_1\lambda_2}, \tag{3.10}$$

and for $\lambda_6 = \lambda_7 = 0$ which ensures the Z_2 symmetry is only softly broken in the potential as is assumed for the rest of this thesis:

$$\lambda_3 + \lambda_4 - |\lambda_5| > -\sqrt{\lambda_1\lambda_2}. \tag{3.11}$$

With these constraints on the λ_i's, the vacuum of the Higgs potential $\Phi_1^\dagger\Phi_1 + \Phi_2^\dagger\Phi_2 = \frac{v^2}{2}$ is the global minimum. Recall that the λ_i's are related to the masses m_h, m_H, m_A and $m_{H^\pm}$ in the physical basis by equations (3.7), (3.3) and (3.4), so this puts constraints on the masses of the Higgs particles.

3.2.2 Tree-level unitarity

The scattering matrix S describing the probability of transitioning from an initial state I to a final state F must respect unity, that is:

$$S^\dagger S = 1,$$

which is to say that the probability of either going to state F, in whatever way, or not, must sum to one. The λ_i couplings in (3.1) appear in the elements of the scattering matrices $S_{Y,\Sigma}$ for a given hypercharge Y and weak isospin Σ and the tree-level unitarity constraint requires that the eigenvalues L_i of $S_{Y,\Sigma}$ be: $|L_i| < 16\pi$. This puts bounds on the λ_i's that can be calculated and checked with 2HDMC.

3.2.3 Perturbativity

Perturbativity requires that the quartic self-couplings of and between the Higgs scalars $\lambda_{\phi_i\phi_j\phi_k\phi_l}$ (for example $\lambda_{hhhh},\ \lambda_{hHHH}$ etc.) not be too large. This stems from the requirement that the theory should be able to be described perturbatively. The quartic couplings

[9] For a more thorough description see for example [9] or [11].

of the physical Higgs fields are related to the λ_i's in the generic basis by (3.8) and (3.9) if expanded in the generic potential (3.1). The requirement puts bounds on λ_i of the quartic couplings in the generic potential in (3.1) in order to keep a typical loop factor $\frac{\lambda^2_{\phi_i\phi_j\phi_k\phi_l}}{16\pi^2} < 1$.

4 Yukawa interactions

In analogy with Eq. (2.11), the 2HDM Yukawa Lagrangian in the generic basis for the first generation can be written:

$$-\mathcal{L}_Y = \overline{Q}_L(Y_1^d\Phi_1 + Y_2^d\Phi_2)d_R + \overline{Q}_L(Y_1^u\tilde{\Phi}_1 + Y_2^u\tilde{\Phi}_2)u_R + \overline{L}(Y_1^l\Phi_1 + Y_2^l\Phi_2)e_R + \text{h.c.} \quad (4.1)$$

Where $\overline{Q}_L = (\overline{u}_L, \overline{d}_L)$, $\overline{L} = (\overline{\nu}_e, \overline{e}_L)$, the $Y^f_{1,2}$ are Yukawa couplings in the generic basis and $\tilde{\Phi}_i = -i\tau_2\Phi_i^*$. For the other generations the same Lagrangian apply if the substitutions $u \to c,\ t$, $d \to s,\ b$ and $e \to \mu,\ \tau$ are made. From equation (3.2) it is evident that the doublets can be rotated to a basis where only one of the doublets gets a non-zero vev. In this basis, called the Higgs basis, the new doublets are denoted H_1 and H_2 and are related to the generic doublets Φ_1 and Φ_2 by a rotation:

$$H_1 = \cos\beta\Phi_1 + \sin\beta\Phi_2 \quad (4.2)$$

$$H_2 = -\sin\beta\Phi_1 + \cos\beta\Phi_2 \quad (4.3)$$

or inverted:

$$\Phi_1 = \cos\beta H_1 - \sin\beta H_2 \quad (4.4)$$

$$\Phi_2 = \sin\beta H_1 + \cos\beta H_2 \quad (4.5)$$

The Yukawa Lagrangian (4.1) in the Higgs basis is obtained by simply replacing

$$Y_1^f\Phi_1 + Y_2^f\Phi_2 = \kappa^f H_1 + \rho^f H_2, \quad (4.6)$$

κ^f and ρ^f are the couplings to fermion f in the Higgs basis.

Expressing Φ_1 and Φ_2 in terms of the physical fields as in (3.8) and (3.9) and inserting into (4.2), (4.3) and repeating for each family gives the Yukawa Lagrangian expressed in terms of the physical fields in the Higgs basis given below in Eq. (4.7).

The Yukawa part of the 2HDM Lagrangian is suitably expressed in terms of the physical fields h, H, A and $H^\pm$. Fermions are denoted as vectors in flavour space $D = (d, s, b)^T$ for down-type quarks, $U = (u, c, t)^T$ for up-type quarks, $L = (e, \mu, \tau)^T$ (in flavour space, not the same L as in (4.1) where only one generation was considered) and $\bar{\nu} = (\bar{\nu_e}, \bar{\nu_\mu}, \bar{\nu_\tau})$ for neutrinos. This Yukawa Lagrangian does not contain any mass term for neutrinos and so they are assumed massless.[10]

[10] A discussion of the implications of massive neutrinos to 2HDM is thus left for further investigations.

The Yukawa Lagrangian can then be written as:

$$\begin{aligned}-\mathcal{L}_{\text{Yukawa}} =&\frac{1}{\sqrt{2}}\overline{D}\Big\{\kappa^D s_{\beta-\alpha}+\rho^D c_{\beta-\alpha}\Big\}Dh+\frac{1}{\sqrt{2}}\overline{D}\Big\{\kappa^D c_{\beta-\alpha}-\rho^D s_{\beta-\alpha}\Big\}DH+\frac{i}{\sqrt{2}}\overline{D}\gamma_5\rho^D DA\\&+\frac{1}{\sqrt{2}}\overline{U}\Big\{\kappa^U s_{\beta-\alpha}+\rho^U c_{\beta-\alpha}\Big\}Uh+\frac{1}{\sqrt{2}}\overline{U}\Big\{\kappa^U c_{\beta-\alpha}-\rho^U s_{\beta-\alpha}\Big\}UH-\frac{i}{\sqrt{2}}\overline{U}\gamma_5\rho^U UA\\&+\frac{1}{\sqrt{2}}\overline{L}\Big\{\kappa^L s_{\beta-\alpha}+\rho^L c_{\beta-\alpha}\Big\}Lh+\frac{1}{\sqrt{2}}\overline{L}\Big\{\kappa^L c_{\beta-\alpha}-\rho^L s_{\beta-\alpha}\Big\}LH+\frac{i}{\sqrt{2}}\overline{L}\gamma_5\rho^L LA\\&+\Big[\overline{U}\{V_{\text{CKM}}\rho^D P_R-\rho^U V_{\text{CKM}}P_L\}DH^+ +\overline{\nu}\rho^L P_R LH^+ +\text{h.c.}\Big].\end{aligned} \tag{4.7}$$

P_R and P_L are the usual projection matrices $P_{R/L}=\frac{1}{2}(1\pm\gamma_5)$. The κ^F $(F=D,\ U,\ L)$ matrices are $\kappa^F=\frac{\sqrt{2}}{v}M^F$ where M^F is the mass matrix in flavour space,

$$M^F=\begin{pmatrix}m_1^F & 0 & 0\\ 0 & m_2^F & 0\\ 0 & 0 & m_3^F\end{pmatrix}$$

The ρ^F matrices determine couplings in the various interactions contained in (4.7) and are model-dependent. In the most general case ρ^F is arbitrary and can thus be non-diagonal. They are free to be determined either by invoking symmetries or general arguments and this is one of the places where different models can be put to test, as many of the interactions described by (4.7) can be measured at high-energy colliders. In this thesis, focus will be on the second row of (4.7), describing the up-quark interactions with neutral Higgs fields.

4.1 Flavour-changing neutral currents

Flavour-changing neutral currents are very restricted by $K^0-\overline{K}^0$ and $B^0-\overline{B}^0$ oscillations [2] and experiments at LHC [4]. For top quark decays, the latest results show $Br(t\to c\phi)<0.79\%$ at 95% confidence level [4]. The fact that FCNCs are observed to be very rare led Glashow and Weinberg [3] to postulate that in 2HDMs, the FCNCs at tree-level are naturally absent due to some symmetry of the theory. The symmetry required is that all fermions of a given charge couple to only one Higgs doublet.

A Z_2 operator is defined with eigenvalues for Φ_1, Φ_2, Q_L and L (as in (4.1)) chosen to be,

$$\begin{aligned}Z_2\Phi_1&=\Phi_1,\\ Z_2\Phi_2&=-\Phi_2,\\ Z_2Q_L&=Q_L,\\ Z_2L&=L.\end{aligned}$$

The $Z_2 f_R$ $(f=u,\ d,\ e)$ eigenvalues are allowed to be different for each fermion-type, the eigenvalues for the right-handed terms can be chosen in eight different ways. Since

a change in all the indices corresponds to a redefinition of $\sin\beta \leftrightarrow \cos\beta$, there are four physically different ways to impose a Z_2 symmetry in a 2HDM. These models are listed in Table 1 in the next section.

Now let us see what happens if a Z_2 symmetry is applied to equation (4.1). Focusing on the first term only:

$$\overline{Q}_L(Y_1^d\Phi_1 + Y_2^d\Phi_2)d_R$$

The eigenvalues for all fields except for d_R have been defined. Assume $Z_2 d_R = d_R$. If this expression is to be invariant under a Z_2 operation, then Y_2^d must be zero since $Z_2\overline{Q}_L Y_2^d\Phi_2 d_R = -\overline{Q}_L Y_2^d\Phi_2 d_R$. If instead $Z_2 d_R = -d_R$, the other term breaks the Z_2 symmetry and so $Y_1^d = 0$ is the only acceptable choice if $\mathcal{L}_y$ is to be symmetric under a Z_2 operation. Depending on what Z_2 eigenvalue d_R is assigned, it may only couple to one of the two doublets. The same thing applies for the other fermion terms in (4.1) (as well as for the other generations). If for example $Y_1^f = 0$ (by imposing a Z_2 symmetry) in (4.6), then the κ^f and ρ^f couplings in the Higgs basis must be proportional to each other:

$$Y_2^f\Phi_2 = \kappa^f H_1 + \rho^f H_2,$$

expanding Φ_2 as in (4.5),

$$\sin\beta Y_2^f H_1 + \cos\beta Y_2^f H_2 = \kappa^f H_1 + \rho^f H_2, \tag{4.8}$$

which implies:

$$\rho^f = \cos\beta Y_2^f = \cot\beta\sin\beta Y_2^f = \kappa^f\cot\beta. \tag{4.9}$$

If instead $Y_2^f = 0$ then,

$$\cos\beta Y_1^f H_1 - \sin\beta Y_1^f H_2 = \kappa^f H_1 + \rho^f H_2, \tag{4.10}$$

$$\Rightarrow \rho^f = -\sin\beta Y_1^f = -\tan\beta\cos\beta Y_1^f = -\kappa^f\tan\beta. \tag{4.11}$$

4.2 2HDM - II

If you follow the approach taken by Glashow and Weinberg [3], the assumption that each type of fermions only couple to one doublet lead to various possibilities of combinations. For example, all quarks and leptons can couple to one doublet (2HDM - I) or the up-type quarks couple to one and the down-type quarks and leptons couple to the other (2HDM - II). All of the models are illustrated in the table below:

Table 1: Different 2HDMs. [9] Caveat: Naming conventions vary a lot in the literature.

Fermion type	2HDM - I	2HDM - II	2HDM LS	2HDM - Flipped	2HDM - III
U	Φ_2	Φ_2	Φ_2	Φ_2	Φ_1, Φ_2
D	Φ_2	Φ_1	Φ_2	Φ_1	Φ_1, Φ_2
L	Φ_2	Φ_1	Φ_1	Φ_2	Φ_1, Φ_2

In order to fulfil the Glashow-Weinberg condition, the ρ^F ($F = U,\ D,\ L$) coupling matrix must be proportional to the κ^F matrices with different proportionality constants depending on which fermions couple to which doublet. In a 2HDM-II, the coupling matrices are:

$$\rho^U = \kappa^U \cot\beta, \quad \rho^D = -\kappa^D \tan\beta, \quad \rho^L = -\kappa^L \tan\beta. \tag{4.12}$$

Since the κ matrices are proportional to the mass matrix and the fields are expressed in the mass basis eigenstate, the requirement $\rho^F \propto \kappa^F$ implies that also the ρ^F matrices are diagonal, i.e. no FCNCs. In this thesis, in order to reduce the number of free parameters present in a completely general 2HDM, the diagonal elements of ρ^U and ρ^D are assumed to be of the 2HDM-II sort, this makes $\tan\beta$ a physical parameter of the theory, whereas in general (2HDM-III), only the difference between the angles $\beta - \alpha$ is a physical observable. The starting point for the model investigated in this thesis is therefore a 2HDM-II but with non-diagonal ρ^F.

4.3 2HDM - III

In a completely general 2HDM - type III, no restrictions on the elements of ρ^F are imposed. However, in order to reduce the number of free parameters some reasonable assumptions can be made. As mentioned in the preceding section, the diagonal elements ρ_{ii} are here assumed to be proportional to the corresponding κ_{ii} elements according to (4.12). In addition, an assumption regarding the off-diagonal FCNC generating elements ρ_{ij} can be made. T.P. Cheng and M. Sher argued in [5] that the assumption made by Glashow-Weinberg in [3] that all the elements of ρ^F in a 2HDM-III should be of the same order of magnitude (set by the heaviest fermion mass) is unreasonable. In the SU(2) generation-model for fermions there is a clear hierarchical structure in the masses of fermions of different generations. The elements of ρ^F are assumed to be proportional to the geometric mean (to make the diagonal elements resemble κ_{ii}) of the quark masses involved.

Qualitatively, the Cheng-Sher ansatz can be summarised as follows: The elements of the coupling matrix ρ^F are,

$$\rho^F_{ij} = \lambda_{ij} \frac{\sqrt{2}}{v} \sqrt{m_i m_j}, \tag{4.13}$$

where m_i and m_j are the masses of fermions of type F and λ_{ij} are constants of order unity (so that the relevant scale is determined by the quark-masses).

The assumptions made so far that will be used when calculating $Br(t \to c\phi)$ are:

1. The diagonal elements of ρ^U and ρ^D are as in a 2HDM-II.
2. The off-diagonal elements of ρ^U are as in the Cheng-Sher ansatz, equation (4.13) with undetermined constants λ_{ij} of order unity.
3. The couplings between anti-quarks and quarks are assumed to be the same $\rho_{ct} = \rho_{tc}$.
4. Only FCNC between the heaviest quarks are considered, meaning all ρ_{ij} are small compared to ρ_{ct} and thus are neglected $\rho_{ij} \approx 0$ except ρ_{ct}.

After all assumptions made, the ρ^U matrix is:

$$\rho^U = \frac{\sqrt{2}}{v}\begin{bmatrix} m_u \cot\beta & 0 & 0 \\ 0 & m_c \cot\beta & \lambda_{ct}\sqrt{m_c m_t} \\ 0 & \lambda_{ct}\sqrt{m_t m_c} & m_t \cot\beta \end{bmatrix}. \tag{4.14}$$

In the plots for the branching ratios illustrated in Section 6, λ_{ct} is varied between $0.1 \leq \lambda_{ct} \leq 10$ and the effect on $Br(t \to c\phi)$ is observed.

4.4 Top quark decay

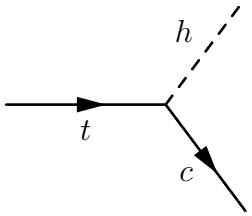

Figure 1: Feynman diagram for top quark decay to a charm quark and a neutral scalar

The decay width $\Gamma(t \to c\phi)$, $(\phi = h,\ H,\ A)$ for the process in Figure 1 is given by [12]:

$$\Gamma(t \to c\phi) = \frac{g_\phi^2}{16\pi} m_t[(1 \pm x_c)^2 - x_\phi^2] \cdot \sqrt{1-(x_\phi + x_c)^2}\sqrt{1-(x_\phi - x_c)^2} \tag{4.15}$$

Where $\pm$ is $+$ for the CP-even scalars $(h,\ H)$ and $-$ for the CP-odd (A). Furthermore g_ϕ is $g_h = -\frac{1}{\sqrt{2}}\rho_{ct}\cos(\beta-\alpha)$, $g_H = \frac{1}{\sqrt{2}}\rho_{ct}\sin(\beta-\alpha)$ and $g_A = \frac{i}{\sqrt{2}}\rho_{ct}\gamma_5$. With kinematic factors $x_c = \frac{m_c}{m_t}$, $x_\phi = \frac{m_\phi}{m_t}$. A derivation of this expression is shown in Appendix A. Neglecting the small term $x_c \approx 0.008$ it is seen that the decay width behaves approximately as a quartic polynomial in x_ϕ (and quadratic in g_ϕ):

$$\Gamma(t \to c\phi) \approx \frac{g_\phi^2}{16\pi} m_t (1 - x_\phi^2)^2\,, \quad (x_c \approx 0). \tag{4.16}$$

In the Section 6 $Br(t \to c\phi)$, which is simply $\Gamma(t \to c\phi)$ in equation (4.15) divided by the total decay width of the top quark, is investigated. Of particular interest is; What values of the couplings, the masses and $\sin(\beta-\alpha)$ are allowed under the theoretical constraints described in Section 3.2 and constraints on $\sin(\beta-\alpha)$ and $\tan\beta$ coming from the properties of the ϕ boson found at LHC [1] to be described in Section 5 as well as how this compares to the experimental restriction that $Br(t \to c\phi) < 0.79\%$? The 2HDMC code has been upgraded in order to calculate FCNCs of the sort $q_i \to q_j\phi$ and the results are presented for the two cases $m_h = 125$ GeV/c^2 and $m_H = 125$ GeV/c^2.

5 Experimental restrictions on $\sin(\beta - \alpha)$

The two most important channels for Higgs discovery at the LHC are the $\phi \to \gamma\gamma$ and $\phi \to ZZ \to 4l$[11] processes shown in Fig. 2, 3 and 4 [13]. In addition to production by $gg \to \phi$, the Higgs boson can also be produced by $W^+W^- \to \phi$, but in this first investigation the latter is neglected and only the former, dominant production channel will be considered [13]. The signal strength for a process with initial state I going to a final state F is defined as,

$$\mu = \frac{\sigma(I \to F)_{observed}}{\sigma(I \to F)_{\mathrm{SM}}}. \tag{5.1}$$

Experimentally found values of the signal strengths corresponding to these processes can be used to put limits on $\sin(\beta - \alpha)$ and $\tan\beta$. Much work has already been devoted to checking the allowed parameter space for $\sin(\beta-\alpha)$ versus $\tan\beta$ (see for example [14] for a thorough investigation) but recent updated values from LHC for the signal strengths [15] motivates an updated analysis.

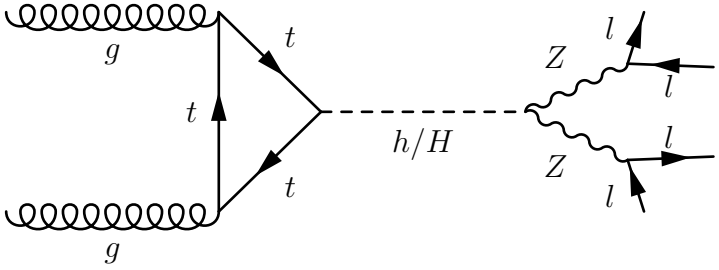

Figure 2: Feynman diagram for $gg \to h/H \to 4l$

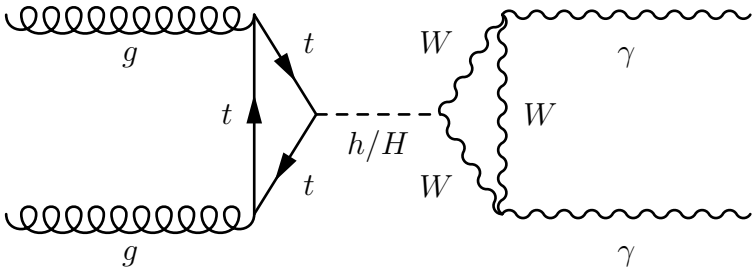

Figure 3: Feynman diagram for $gg \to h/H \to \gamma\gamma$ through a W-loop.

[11] Throughout this section, $\phi = h$ or H will refer only to the found Higgs boson in the respective cases.

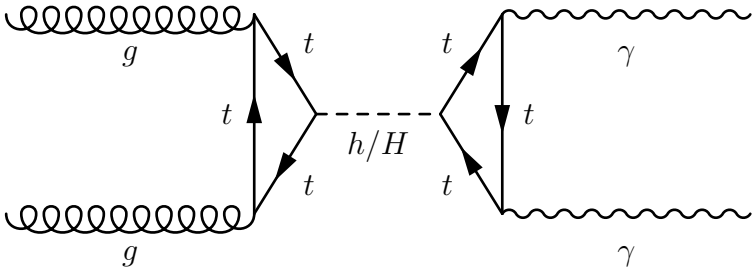

Figure 4: Feynman diagram for $gg \to h/H \to \gamma\gamma$ through a top-loop.

If the 2HDM should correspond to the observed data, then

$$\frac{\sigma(I \to F)_{\text{2HDM}}}{\sigma(I \to F)_{\text{SM}}} = \mu = \frac{\sigma(I \to F)_{\text{observed}}}{\sigma(I \to F)_{\text{SM}}}. \tag{5.2}$$

The signal strength μ_{hZZ} (μ_{HZZ}) can be calculated and compared to experimental data. With the approximation that $gg \to \phi$ production via a top-loop dominates [13],

$$\mu_{\phi ZZ} = \frac{\sigma(p\bar{p} \to \phi)_{\text{2HDM}}}{\sigma(p\bar{p} \to \phi)_{\text{SM}}} \cdot \frac{Br(\phi \to ZZ)_{\text{2HDM}}}{Br(\phi \to ZZ)_{\text{SM}}} \tag{5.3}$$

$$\approx \left(\frac{g^{\phi tt}_{\text{2HDM}}}{g^{\phi tt}_{\text{SM}}}\right)^2 \cdot \frac{\Gamma(\phi \to ZZ)_{\text{2HDM}}}{\Gamma(\phi \to ZZ)_{\text{SM}}} \cdot \frac{\Gamma^{\text{TOT}}_{\text{SM}}}{\Gamma^{\text{TOT}}_{\text{2HDM}}} \tag{5.4}$$

$$= \left(\frac{g^{\phi tt}_{\text{2HDM}}}{g^{\phi tt}_{\text{SM}}}\right)^2 \cdot \left(\frac{g^{\phi ZZ}_{\text{2HDM}}}{g^{\phi ZZ}_{\text{SM}}}\right)^2 \cdot \frac{\Gamma^{\text{TOT}}_{\text{SM}}}{\Gamma^{\text{TOT}}_{\text{2HDM}}}. \tag{5.5}$$

So far this is completely general and true for both μ_{hZZ} and μ_{HZZ}. The signal strength $\mu_{\phi\gamma\gamma}$, corresponding to $\phi \to \gamma\gamma$, through the processes shown in Fig. 3 and 4 is,

$$\mu_{\phi\gamma\gamma} = \frac{\sigma(p\bar{p} \to \phi)_{\text{2HDM}}}{\sigma(p\bar{p} \to \phi)_{\text{SM}}} \cdot \frac{Br(\phi \to \gamma\gamma)_{\text{2HDM}}}{Br(\phi \to \gamma\gamma)_{\text{SM}}} \tag{5.6}$$

$$\approx \left(\frac{g^{\phi tt}_{\text{2HDM}}}{g^{\phi tt}_{\text{SM}}}\right)^2 \cdot \frac{Br(\phi \to \gamma\gamma)_{\text{2HDM}}}{Br(\phi \to \gamma\gamma)_{\text{SM}}}. \tag{5.7}$$

For the case $\phi = h$ in a 2HDM-II from Eq. (4.7) and (4.12):

$$\frac{g^{htt}_{\text{2HDM}}}{g^{htt}_{\text{SM}}} = \frac{\cos\alpha}{\sin\beta}, \tag{5.8}$$

and for $\phi = H$,

$$\frac{g^{Htt}_{\text{2HDM}}}{g^{Htt}_{\text{SM}}} = \frac{\sin\alpha}{\sin\beta}. \tag{5.9}$$

The h coupling to the Z-boson is [11]:

$$\frac{g^{hZZ}_{\text{2HDM}}}{g^{hZZ}_{\text{SM}}} = \sin(\beta - \alpha). \tag{5.10}$$

and for H,

$$\frac{g^{HZZ}_{\text{2HDM}}}{g^{HZZ}_{\text{SM}}} = \cos(\beta - \alpha). \tag{5.11}$$

To compare $\frac{\Gamma^{\text{TOT}}_{\text{SM}}}{\Gamma^{\text{TOT}}_{\text{2HDM}}}$ to experimental data, $\Gamma^{\text{TOT}}_{\text{SM}}$ is obtained from a tabulated reference [13]. The Higgs Cross-Section group has also calculated all partial Higgs decay widths and branching ratios in the Standard Model [13] so these values are inserted immediately in Eq. (5.4) and (5.7) and the 2HDM decays $\Gamma^{\text{TOT}}_{\text{2HDM}}$ and branching ratio $Br(\phi \to \gamma\gamma)_{\text{2HDM}}$ are calculated using 2HDMC.

An approximate analytic formula for $\mu_{\phi ZZ}$ can also be obtained. This approach might be useful to give an idea of how $\mu_{\phi ZZ}$ behaves as a function of $\tan\beta$ and $\sin(\beta - \alpha)$.

The Higgs boson mostly decays to $b\bar{b}$ [13] and for a 2HDM-II in the case $\phi = h$:

$$\frac{g^{hbb}_{\text{2HDM}}}{g^{hbb}_{\text{SM}}} = \frac{\sin\alpha}{\cos\beta}. \tag{5.12}$$

So if $\frac{\Gamma^{\text{TOT}}_{\text{SM}}}{\Gamma^{\text{TOT}}_{\text{2HDM}}}$ is approximated to its dominating channel,

$$\frac{\Gamma^{\text{TOT}}_{\text{SM}}}{\Gamma^{\text{TOT}}_{\text{2HDM}}} \approx \frac{\Gamma^{hbb}_{\text{SM}}}{\Gamma^{hbb}_{\text{2HDM}}} = \left(\frac{g^{hbb}_{\text{SM}}}{g^{hbb}_{\text{2HDM}}}\right)^2 = \left(\frac{\cos\beta}{\sin\alpha}\right)^2, \tag{5.13}$$

this gives the following expression for μ_{hZZ}:

$$\mu_{hZZ} \approx \frac{\sin^2(\beta - \alpha)}{\tan^2\alpha \tan^2\beta}. \tag{5.14}$$

As for the case $\phi = H$, the same approximation apply, with the change

$$\frac{g^{Hbb}_{\text{2HDM}}}{g^{Hbb}_{\text{SM}}} = \frac{\cos\alpha}{\cos\beta}\,. \tag{5.15}$$

Leading to

$$\mu_{HZZ} \approx \frac{\cos^2(\beta - \alpha)\tan^2\alpha}{\tan^2\beta}. \tag{5.16}$$

The process $\phi \to \gamma\gamma$ can happen through two processes, shown in Fig. 3 and 4. However, the two channels interfere giving linear terms in $\cos(\beta - \alpha)$, so no simple approximate analytic formula for $\mu_{\gamma\gamma}$ can be obtained.

6 Results and discussion

In the following, the results obtained using 2HDMC will be presented. The 2HDM under consideration, after all assumptions, still contains free parameters and some of them will simply be chosen to have a fixed value $(m^2_{12}, m_A, m_{H^\pm})$ accepted by all the theoretical constraints, whereas others are varied $(m_h, m_H, \sin(\beta - \alpha), \tan\beta)$ in the different plots

presented throughout this section. The values for the parameters that are fixed as well as the different m_h and m_H values that are used in the plots are presented in Table 2.

Table 2: Parameter values used in the different cases, the masses of m_h and m_H, $\tan\beta$ and $\sin(\beta-\alpha)$ will be stated explicitly in each plot. Every mass term in the table is given in units GeV/c^2.

Parameter	Case $m_h = 125$ GeV/c^2	Case $m_H = 125$ GeV/c^2
m_h =	125	75, 95, 115
m_H =	400	125
m_A =	500	500
$m_{H^\pm}$ =	500	500
m_{12}^2 =	500	500

The fixed mass parameters (m_{12}^2, m_A, $m_{H^\pm}$) are chosen to not give trouble regarding the theoretical constraints of section 3.2 but also to be heavy enough to not affect other Higgs decay widths at tree-level. If a more thorough analysis would be made, for example using the programs HiggsBounds [16] and HiggsSignals [17], specific masses with the given parameters that give acceptable values for observables (within measured values) could be found. In this investigation, the mass terms are just chosen to be heavy to not enter any of the illustrated decays. There is one exception that needs to be treated with care. In the heavy found Higgs case, the light Higgs can obviously not be made any heavier than 125 GeV/c^2. In this case its effects on all measured observables need to be calculated, this has been done in [14] and they found acceptable points for m_h. In this investigation, the experimental dependence on m_h in the heavy found Higgs case is excluded, and this means that the points (y_1, y_2 and y_3) chosen in Fig. 8 might not necessarily be acceptable if all measured observables are calculated. However, the approach has been to illustrate the dependence of $Br(t \to c\phi)$ on $\sin(\beta-\alpha)$. Even if precisely these points aren't physically acceptable, as shown in [14] some points in the near region can be found that are.

6.1 Allowed values for $\sin(\beta-\alpha)$

With the mass terms fixed according to Table 2, the only free parameters left are λ_{ct}, $\sin(\beta-\alpha)$ and $\tan\beta$. The last two are related to each other through the signal strengths $\mu_{\gamma\gamma}$ and μ_{ZZ} as discussed in Section 5. Fig. 5 and 6 show the allowed regions after imposing the 68% confidence level (CL) constraints $0.90 < \mu_{\gamma\gamma} < 1.43$ (red area) and $1.15 < \mu_{ZZ} < 1.70$ (green area) as the signal strengths have been measured in [15] for the two cases m_h or m_H found respectively. The blue area corresponds to the overlap, where both restrictions are satisfied.

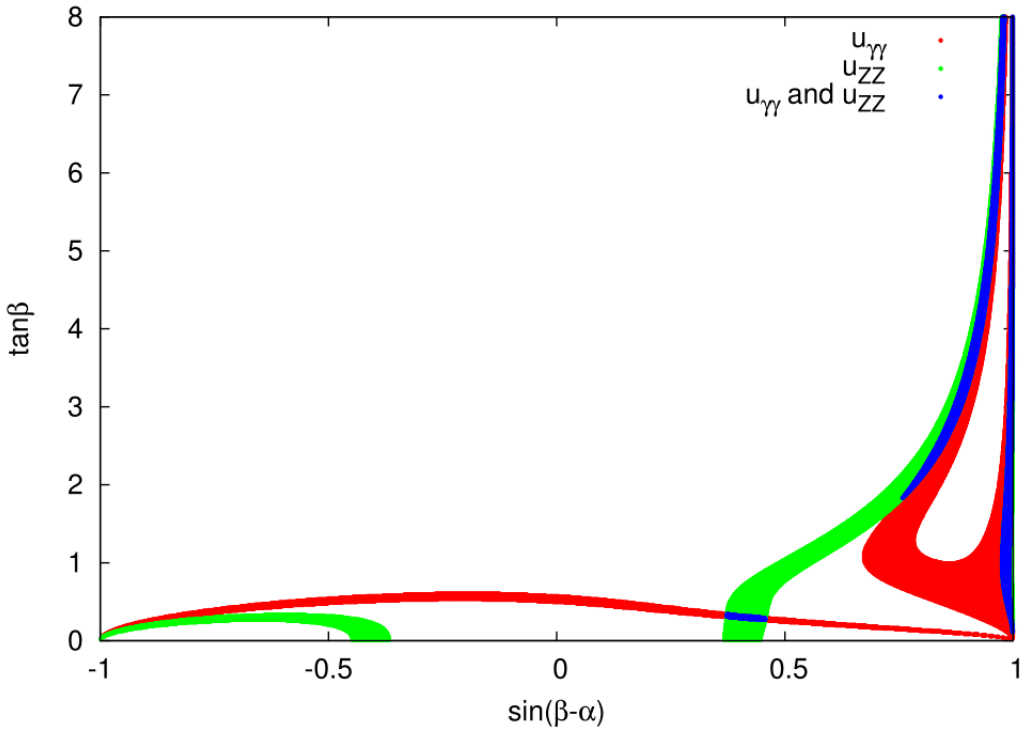

Figure 5: Allowed values for $\tan\beta$ and $\sin(\beta-\alpha)$ based on the signal strengths $\mu_{\gamma\gamma}$ and μ_{ZZ} in the case $m_h = 125\,\mathrm{GeV}/c^2$.

The limit $\sin(\beta-\alpha) \to 1$ is called the alignment limit [14], in which the couplings to the found Higgs boson becomes exactly as in the Standard Model. When this happens, the model can still have two neutral CP-even scalars, but their couplings to fermions are not related to each other in the general case[12]. In the $m_H = 125\,\mathrm{GeV}/c^2$ case, the alignment limit corresponds to $\cos(\beta-\alpha) \to 1$ or $\sin(\beta-\alpha) \to 0$. The sign of $\sin(\beta-\alpha)$ depends on how the angle α is defined and may differ from conventions used in other articles.

The parameter-space shown in Fig. 6 does not depend on m_h (as long as $2m_h > m_H$, to prevent the decay $H \to hh$) so the blue area shown there is a valid region with the given parameters for all values of m_h in the range $\frac{m_H}{2} < m_h < m_H$ shown in Fig. 8. In fact, all the allowed parameter regions in Fig. 5 and 6 are independent of any mass term, as listed in Table 2 (apart from the found Higgs boson mass at 125 GeV/c^2). The effects of imposing the theoretical constraints from section 3.2 are shown in Fig. 7 and 8. Note that this introduces a dependence on the masses of the other Higgs bosons as explained in more detail below.

[12]That is, in a Type - III. In a Z_2 conserving 2HDM, they can still be related by the relations in Eq. (4.12).

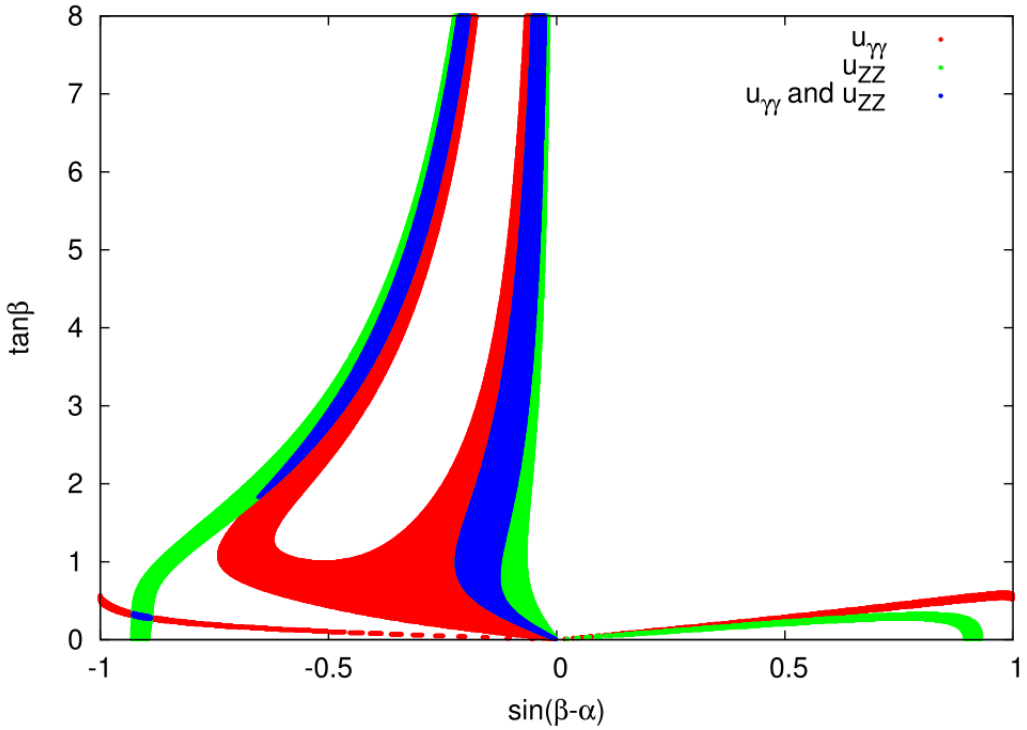

Figure 6: Allowed values for $\tan\beta$ and $\sin(\beta-\alpha)$ based on the signal strengths $\mu_{\gamma\gamma}$ and μ_{ZZ} in the case $m_H = 125\,\mathrm{GeV}/c^2$.

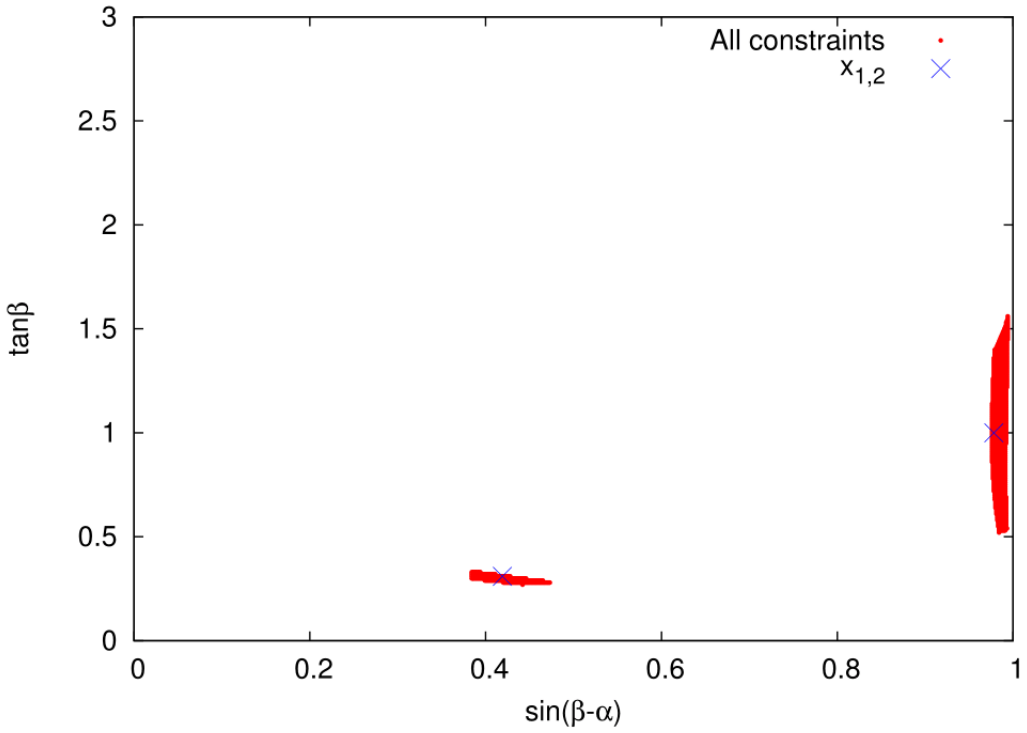

Figure 7: Allowed values for $\tan\beta$ and $\sin(\beta-\alpha)$ in case $m_h = 125\,\mathrm{GeV}/c^2$ after imposing both experimental and theoretical constraints as explained in the text.

The parameter-space in Fig. 7 and 8 is restricted by both $\mu_{\gamma\gamma}$, μ_{ZZ} and all theoretical constraints (vacuum stability, tree-level unitarity and perturbativity). In order to illustrate the dependence of $Br(t \to c\phi)$ on $\sin(\beta-\alpha)$, two points x_1 and x_2 in Fig. 7 (from left to right, respectively) have been picked, one from each region. They are highlighted with blue crosses at $x_1 = (\sin(\beta-\alpha)_1,\ \tan\beta_1) = (0.419,\ 0.31)$ and $x_2 = (0.978,\ 1)$. These points will be used later when calculating the branching ratios in Fig. 10. For case $m_H = 125\,\mathrm{GeV}/c^2$ as illustrated in Fig. 8, three points y_1, y_2 and y_3 have been picked, one in each region (again from left to right). These points are used in the calculation of branching ratios in this heavy found Higgs case, as illustrated in Fig. 11, 12 and 13: $y_1 = (-0.901,\ 0.3)$, $y_2 = (-0.329,\ 4.81)$ and $y_3 = (-0.168,\ 2)$. These points have been chosen deliberately to be allowed in all the illustrated cases $m_h = 75\,\mathrm{GeV}/c^2$, $m_h = 95\,\mathrm{GeV}/c^2$ and $m_h = 115\,\mathrm{GeV}/c^2$.

When the theoretical constraints (as described in 3.2) are applied as in Fig. 7 and 8, the allowed parameter region does depend on the masses since the constraints on the couplings λ_i's in the generic basis are related to the physical masses through equations (3.7), (3.3) and (3.4). This means that if also the other mass terms would be varied, more allowed parameter points could be found and the red region in Fig. 7 and 8 would expand. For the given set of mass terms, perturbativity imposes the strongest constraint and is responsible

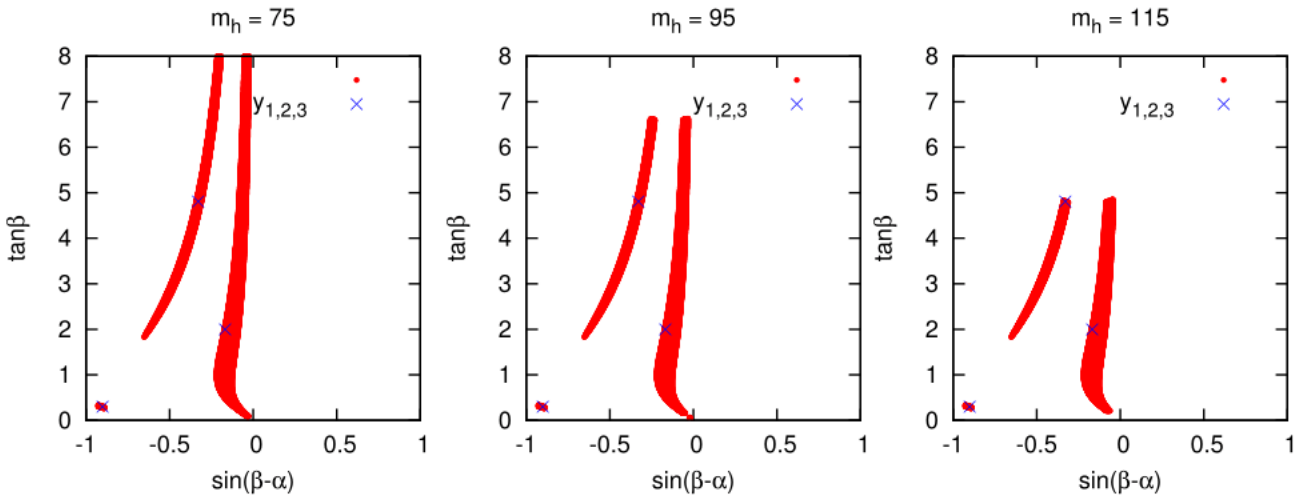

Figure 8: Allowed values for $\tan\beta$ and $\sin(\beta-\alpha)$ in case $m_H = 125\,\mathrm{GeV}/c^2$ after imposing both experimental and theoretical constraints as explained in the text.

for much of the vanished region for increasing m_h in Fig. 8.

The branching ratio $Br(t \to c\phi)$ doesn't depend on $\tan\beta$ so any point along a vertical line (within the red area) could have been chosen in Fig. 7 and 8. This is particularly interesting in Fig. 8 since the allowed parameter region removed by the theoretical constraints for larger m_h mostly correspond to higher values of $\tan\beta$ and doesn't affect the allowed values of $\sin(\beta-\alpha)$ very much, at least in the region $0 < \tan\beta < 8$ that is observed.

Data from $B-\overline{B}$ meson mixing and R_b[13] measurements [18] forces $\tan\beta \gtrsim 1$ unless $m_{H^\pm}$ is quite heavy. This is another reason why $m_{H^\pm}$ was chosen to be heavy in Table 2. As seen in Fig. 9 below, slightly lower values than $\tan\beta = 1$ are allowed for $m_{H^\pm} = 500$ GeV/c^2 at 95% CL but it is doubtful if the points x_1 in Fig. 7 and y_1 in Fig. 8 are allowed. They have been included anyway for illustrative purposes.

[13] $R_b \equiv \Gamma(ZZ \to b\bar{b})/\Gamma(ZZ \to \text{hadrons})$ [18].

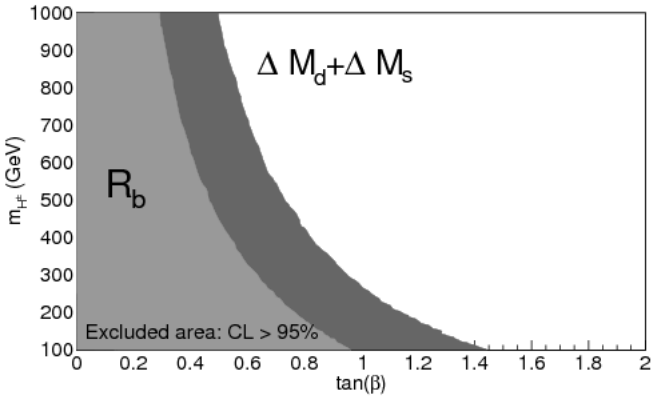

Figure 9: Constraints on $(\tan\beta,\ m_{H^\pm})$ from $B-\overline{B}$ mixing and R_b data in Type II. Picture obtained from [14].

6.2 Branching ratio $Br(t \to c\phi)$

Now that a few parameter-points for $\sin(\beta-\alpha)$ accepted by measurements and theoretical constraints have been found, the branching ratios for $t \to c\phi$ in the different cases can be calculated. The still undetermined Yukawa coupling λ_{ct} is varied between $0.1 < \lambda_{ct} < 10$ in the figures below. The results are illustrated in Fig. 10 in the light found Higgs case for two different values of $\sin(\beta-\alpha)$ to illustrate the dependence and show what ranges of $Br(t \to c\phi)$ when λ_{ct} is varied that these points correspond to. In the heavy found Higgs case, as mentioned earlier, the undiscovered light Higgs boson must also enter the top decay. In addition to the dependence on $\sin(\beta-\alpha)$ illustrated for the three points y_1, y_2 and y_3 in each figure Fig. 12, 11 and 13, the dependence for $Br(t \to ch)$ on m_h (in the range $\frac{m_H}{2} < m_h < m_H$) for three different values of m_h are illustrated in the respective different figures. In all of the plots, the experimental limit $Br(t \to c\phi) < 0.79\%$ at 95% CL as measured in [4] is illustrated as a horizontal line. Note that this limit is only valid for the found Higgs boson, as will be discussed below. According to the Cheng-Sher ansatz discussed in Section 4.3, the constant λ_{ct} should be of order unity. In the figures throughout this section, the effects from the experimental limit on this assumption will be illustrated and discussed.

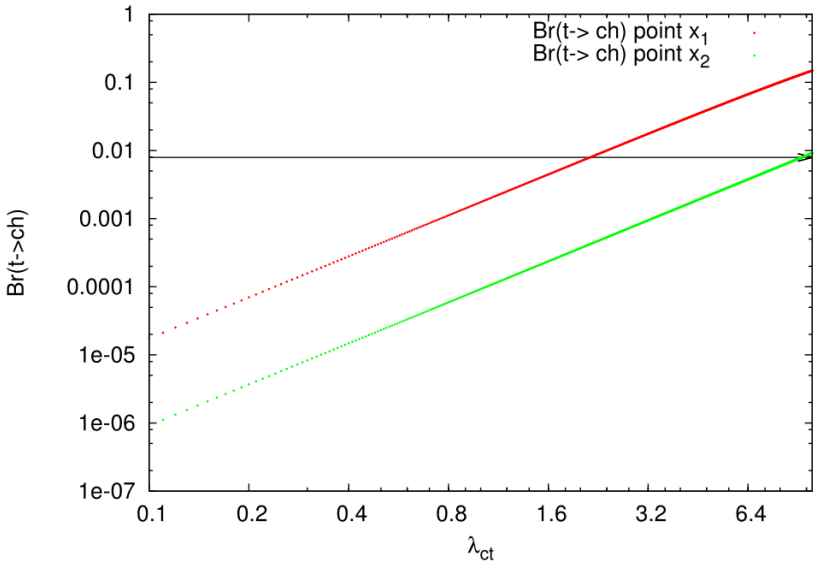

Figure 10: Branching ratio for $t \to ch$ in case $m_h = 125\,\mathrm{GeV}/c^2$ for the different parameter points $x_1 = (0.419,\ 0.31)$ and $x_2 = (0.978,\ 1)$.

As seen in Fig. 10, λ_{ct} can be of order $\mathcal{O}(1)$ without conflicting with experiments in the light found Higgs case. In the more probable close-to alignment limit (x_2 because of the $\tan\beta \gtrsim 1$ restriction in Fig. 9 from [14]) the experiment at [4] has just barely excluded the largest allowed value of $\lambda_{ct} \lesssim 10$. For the points x_1 (x_2) the experimental limit corresponds to forcing $\lambda_{ct} < 2.1$ ($\lambda_{ct} < 9.2$).

The alignment limit to the Standard Model Higgs boson (with absence of FCNCs at tree-level) can be seen in Fig. 10, as $\sin(\beta-\alpha) \to 1$ (x_2 compared to x_1) and $Br(t \to ch) \to 0$ since $g_h = -\frac{1}{\sqrt{2}}\rho_{ct}\cos(\beta-\alpha) \to 0$ in equation (4.15). The same thing happens in case $m_H = 125$ GeV$/c^2$ in Fig. 11, 12 and 13 for $g_H \propto \sin(\beta-\alpha) \to 0$ (y_3 compared to y_1), but FCNCs involving the undiscovered Higgs boson h can still occur in this case since it couples to the general ρ matrices when $\cos(\beta-\alpha) = 1$.

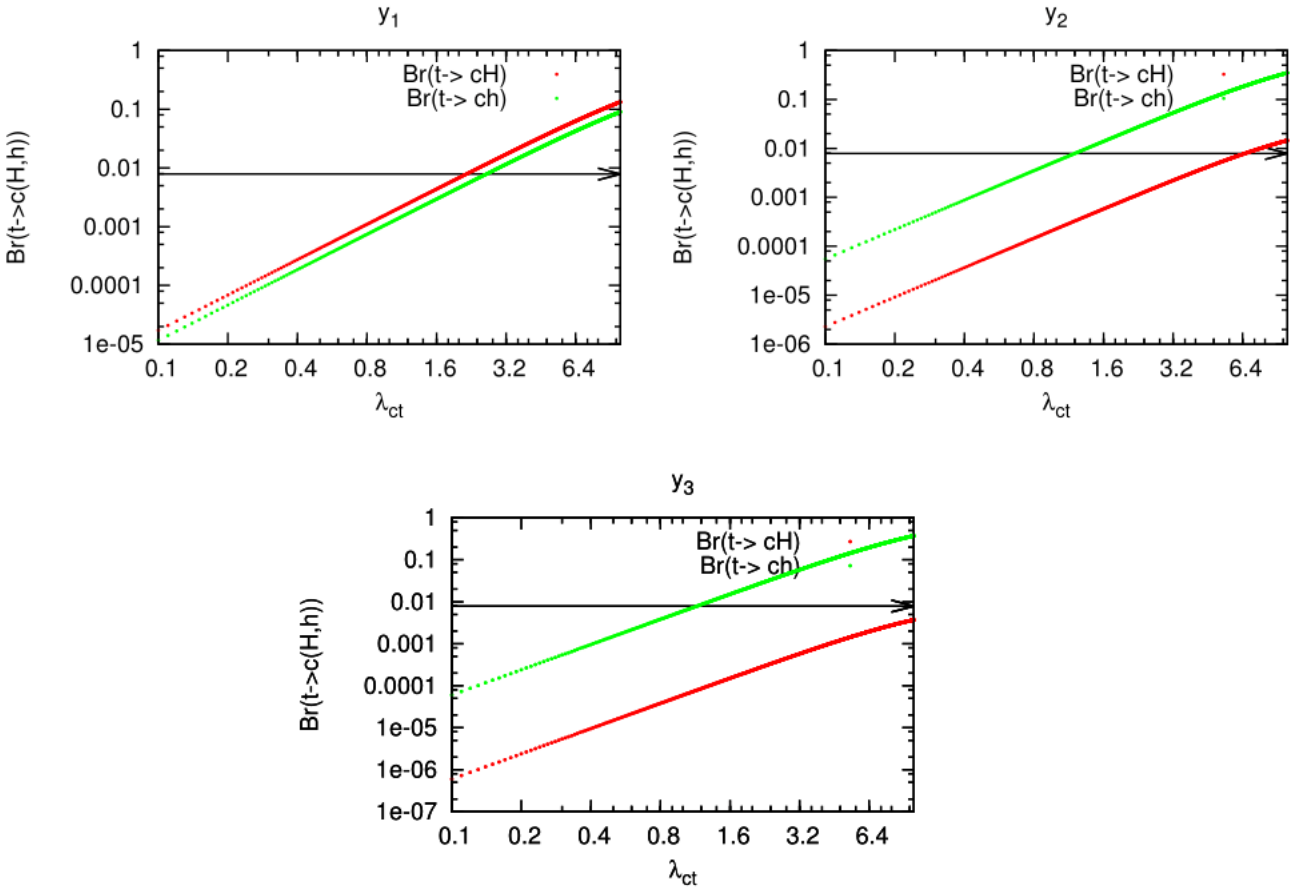

Figure 11: Branching ratio for $t \to c(H,h)$ in case $m_H = 125\,\mathrm{GeV}/c^2$ and $m_h = 75\,\mathrm{GeV}/c^2$ for the different parameter points $y_1 = (-0.901,\ 0.3)$, $y_2 = (-0.329,\ 4.81)$ and $y_3 = (-0.168,\ 2)$.

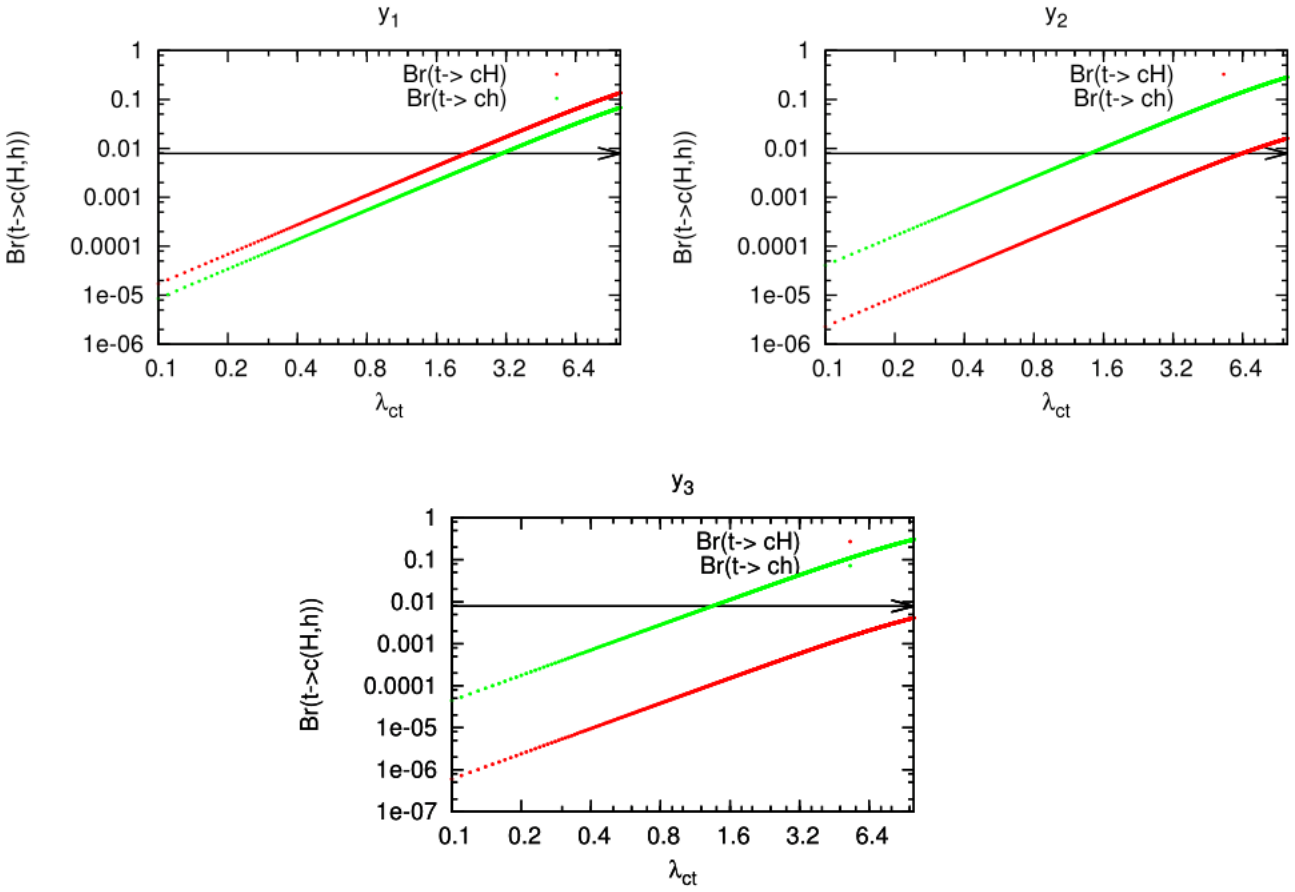

Figure 12: Branching ratio for $t \to c(H,h)$ in case $m_H = 125\,\mathrm{GeV}/c^2$ and $m_h = 95\,\mathrm{GeV}/c^2$ for the different parameter points $y_1 = (-0.901,\ 0.3)$, $y_2 = (-0.329,\ 4.81)$ and $y_3 = (-0.168,\ 2)$.

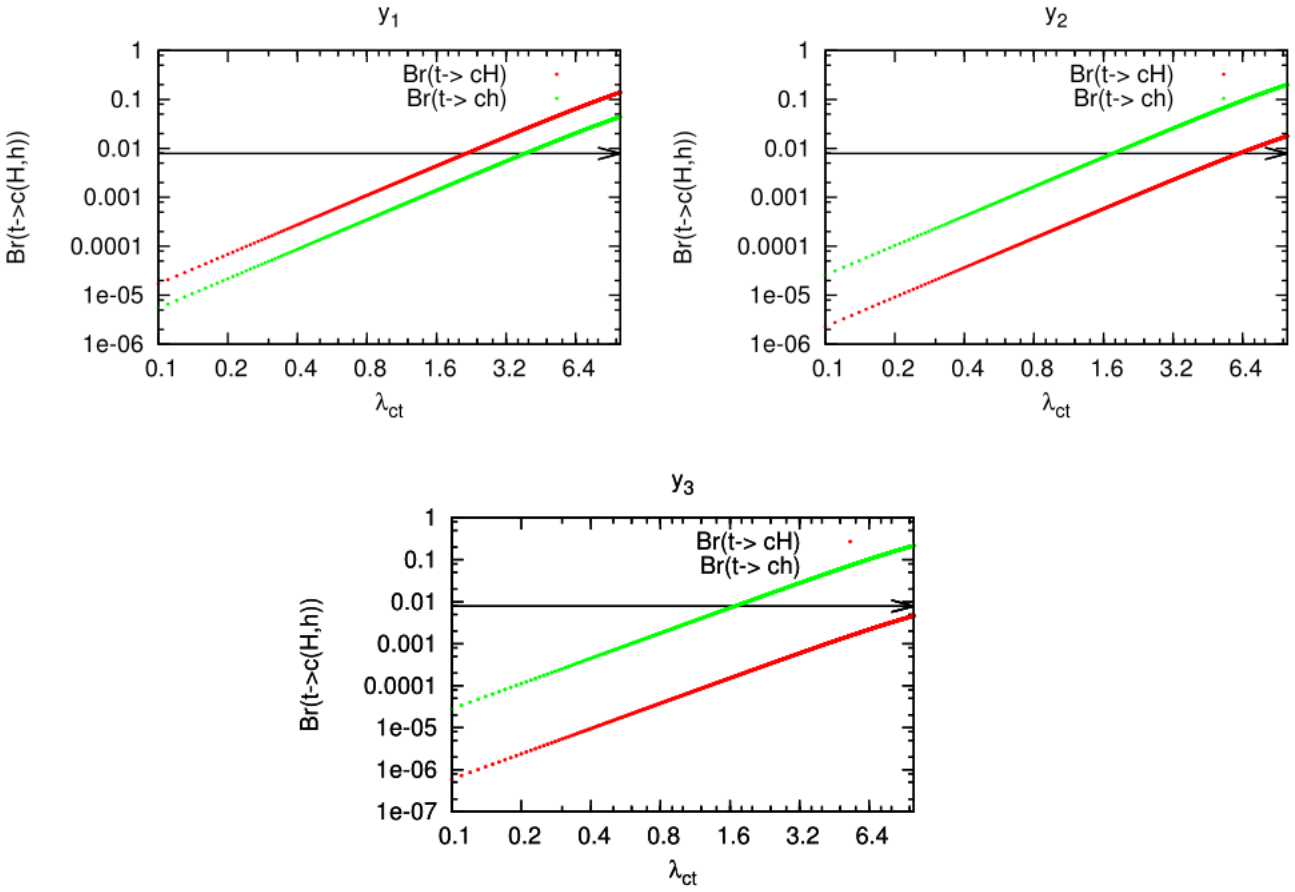

Figure 13: Branching ratio for $t \to c(H,h)$ in case $m_H = 125\,\mathrm{GeV}/c^2$ and $m_h = 115\,\mathrm{GeV}/c^2$ for the different parameter points $y_1 = (-0.901,\ 0.3)$, $y_2 = (-0.329,\ 4.81)$ and $y_3 = (-0.168,\ 2)$.

The restrictions on λ_{ct} in the heavy found Higgs case for the various values of m_h and $\sin(\beta-\alpha)$ are summarized in Table 3. It is seen that λ_{ct} can be of order unity in this case, for all parameter points, as well.

Table 3: Limits on λ_{ct} from $Br(t \to cH) < 0.79$ %.

$m_h =$	75	95	115
y_1	$\lambda_{ct} < 2.1$	$\lambda_{ct} < 2.1$	$\lambda_{ct} < 2.1$
y_2	$\lambda_{ct} < 6.5$	$\lambda_{ct} < 6.3$	$\lambda_{ct} < 6.1$
y_3	$\lambda_{ct} < 25$	$\lambda_{ct} < 18$	$\lambda_{ct} < 14$

Something interesting occurs in Fig. 11, 12 and 13. Since the experimental limit $Br(t \to cH) < 0.79$ % as measured in [4] is only obtained for a Higgs mass of $m_H = 125$ GeV/c^2 the channel $Br(t \to ch)$ in the heavy found Higgs case is not taken into account in [4].[14] In Fig. 11, 12 and 13 with (the more probable) angles (y_2, y_3), $Br(t \to ch)$ is even larger than the channel through the found Higgs ($m_H = 125$ GeV/c^2). This implies that an investigation of the kind done in [4] but for a Higgs mass lower than 125 GeV/c^2 and with the corresponding right couplings could be of interest. However, one should note that before such an investigation is started, the allowed mass ranges for m_h and couplings through their effect on other measured observables[15] should be performed, in particular since a low Higgs mass could enter and dangerously affect many observed decays.

7 Conclusions and outlook

To conclude, in this thesis a 2HDM - type III with diagonal elements as in 2HDM - type II under the constraints imposed by vacuum stability, tree-level unitarity and perturbativity has been investigated. It is shown that the allowed region of $\sin(\beta-\alpha)$ is almost independent of the mass of a lighter Higgs boson with $2m_h > m_H$ in the case $m_H = 125$ GeV/c^2 with $0 < \tan\beta < 8$, for a specific set of mass terms, as far as the theoretical constraints are concerned.

In addition, the effect on the model from recent restrictions on top quark related FCNCs in [4] has also been investigated. It has been shown that the experimental restriction on top quark flavour-changing neutral decay $t \to c\phi$ can be accounted for in a 2HDM - III using Cheng-Sher's ansatz, the undetermined coupling λ_{ct} can be of order unity in both cases without conflicting with experiment.

For large $\sin(\beta-\alpha)$ in case the found Higgs boson is the heavy one, the branching ratio for $t \to ch$ is shown to be larger than the branching ratio $Br(t \to cH)$ that was searched for in [4], implying that a similar investigation taking into account the effects of a lighter Higgs boson might be of interest.

[14] In other words, the horizontal line at $Br(t \to cH)$ in Fig. 11, 12 and 13 is only valid for the red line (decay to H).

[15] For example by implementing HiggsBounds [16] and HiggsSignals [17] in 2HDMC and looping over the allowed masses and couplings.

From the limits on the Yukawa coupling, it is clear that acceptable values of the parameters in a 2HDM - III can be found without fine-tuning[16], the experimental limit on $Br(t \to c\phi)$ does not require a 2HDM - III to resort to fine-tuning of its parameters.

Many things could be improved in a further investigation: Since the mass terms involved were chosen quite arbitrarily, a more thorough investigation would include letting the mass terms vary to find more allowed values for $\sin(\beta - \alpha)$ under the constraints of vacuum stability, tree-level unitarity and perturbativity. Such an analysis should make use of tools such as HiggsBounds and HiggsSignals to check how the masses and couplings affect other experimentally measured decays. This restriction would make the allowed region in parameter-space shrink. This is done in [14], but the allowed mass terms are not stated explicitly.

From an experimental perspective, it might be interesting to know in what range of λ_{ct} one might hope to be able to find the decay $t \to c\phi$. Since the statistical error σ in $Br(t \to c\phi)$ falls with the number of points N as $\frac{1}{\sqrt{N}}$, to get an experimental value with 10 times better precision than for example the one in [4], the LHC would have to acquire ~ 100 times more data. The integrated luminosity used in [4] is 20.3 fb^{-1} and one would have to acquire an integrated luminosity of 2000 fb^{-1} which will probably take $\mathcal{O}(10)$ years. This means that if $\lambda_{ct} \lesssim 1$ it is unlikely that the $Br(t \to ch)$ channel ever will be observed in the light found Higgs case or $Br(t \to cH)$ in the heavy found Higgs case according to the model considered in this thesis.

Of greatest interest would be to check if, in case the found Higgs is the heavier, there exist points in $(m_h,\ m_A,\ m_H^{\pm},\ m_{12}^2)$-space acceptable by all measured observables (as can be checked in HiggsBounds) that allows the branching ratio $Br(t \to ch)$ to be detectable. Since the investigation in [4] used the $H \to \gamma\gamma$ decay, it would be necessary (and easily done using 2HDMC) to check the $h \to \gamma\gamma$ with correct couplings and a lower-than-125 GeV/c^2 Higgs mass. In addition, other channels that contributes to unwanted background should be checked, perhaps not even the $h \to \gamma\gamma$ channel is optimal for searches for $t \to ch$ for a lower Higgs mass.

References

[1] **ATLAS** Collaboration, G. Aad et al., *Observation of a new particle in the search for the Standard Model Higgs boson with the ATLAS detector at the LHC*, *Phys.Lett.* **B716** (2012) 1–29, [arXiv:1207.7214].

[2] A. Crivellin, A. Kokulu, and C. Greub, *Flavor-phenomenology of two-Higgs-doublet models with generic Yukawa structure*, *Phys.Rev.* **D87** (2013), no. 9 094031, [arXiv:1303.5877].

[3] S. L. Glashow and S. Weinberg, *Natural Conservation Laws for Neutral Currents*, *Phys.Rev.* **D15** (1977) 1958.

[16] Which would have been the case if the Cheng-Sher ansatz would have broken down, and λ_{ct} would have to be several orders smaller or larger than unity.

[4] **ATLAS** Collaboration, G. Aad et al., *Search for top quark decays $t \to qH$ with $H \to \gamma\gamma$ using the ATLAS detector*, *JHEP* **1406** (2014) 008, [arXiv:1403.6293].

[5] T. Cheng and M. Sher, *Mass Matrix Ansatz and Flavor Nonconservation in Models with Multiple Higgs Doublets*, *Phys.Rev.* **D35** (1987) 3484.

[6] G. L. Kane, *MODERN ELEMENTARY PARTICLE PHYSICS*, .

[7] F. Englert and R. Brout, *Broken Symmetry and the Mass of Gauge Vector Mesons*, *Phys.Rev.Lett.* **13** (1964) 321–323.

[8] P. W. Higgs, *Broken Symmetries and the Masses of Gauge Bosons*, *Phys.Rev.Lett.* **13** (1964) 508–509.

[9] G. Branco, P. Ferreira, L. Lavoura, M. Rebelo, M. Sher, et al., *Theory and phenomenology of two-Higgs-doublet models*, *Phys.Rept.* **516** (2012) 1–102, [arXiv:1106.0034].

[10] D. Eriksson, J. Rathsman, and O. Stal, *2HDMC: Two-Higgs-Doublet Model Calculator Physics and Manual*, *Comput.Phys.Commun.* **181** (2010) 189–205, [arXiv:0902.0851].

[11] J. F. Gunion, H. E. Haber, G. L. Kane, and S. Dawson, *The Higgs Hunter's Guide*, *Front.Phys.* **80** (2000) 1–448.

[12] W.-S. Hou, *Tree level t – c h or h – t anti-c decays*, *Phys.Lett.* **B296** (1992) 179–184.

[13] **LHC Higgs Cross Section Working Group** Collaboration, S. Heinemeyer et al., *Handbook of LHC Higgs Cross Sections: 3. Higgs Properties*, arXiv:1307.1347.

[14] P. Ferreira, R. Guedes, M. O. Sampaio, and R. Santos, *Wrong sign and symmetric limits and non-decoupling in 2HDMs*, *JHEP* **1412** (2014) 067, [arXiv:1409.6723].

[15] **ATLAS, CMS** Collaboration, G. Aad et al., *Combined Measurement of the Higgs Boson Mass in pp Collisions at $\sqrt{s} = 7$ and 8 TeV with the ATLAS and CMS Experiments*, arXiv:1503.07589.

[16] P. Bechtle, O. Brein, S. Heinemeyer, O. Stål, T. Stefaniak, et al., HiggsBounds – 4*: Improved Tests of Extended Higgs Sectors against Exclusion Bounds from LEP, the Tevatron and the LHC*, *Eur.Phys.J.* **C74** (2014), no. 3 2693, [arXiv:1311.0055].

[17] P. Bechtle, S. Heinemeyer, O. Stål, T. Stefaniak, and G. Weiglein, *HiggsSignals: Confronting arbitrary Higgs sectors with measurements at the Tevatron and the LHC*, *Eur.Phys.J.* **C74** (2014), no. 2 2711, [arXiv:1305.1933].

[18] O. Deschamps, S. Descotes-Genon, S. Monteil, V. Niess, S. T'Jampens, et al., *The Two Higgs Doublet of Type II facing flavour physics data*, *Phys.Rev.* **D82** (2010) 073012, [arXiv:0907.5135].

[19] D. Griffiths, *Introduction to elementary particles*, .

A Derivation of the Decay Width for $t \to c\phi$

For a tree-level decay with $A \to B+C$, the decay width Γ is (in natural units $c = \hbar = 1$) [6]:

$$d\Gamma = \frac{1}{(2\pi)^2}\frac{1}{2E_A}\delta^4(P_B + P_C - P_A)\frac{dP_B}{2E_B}\frac{dP_C}{2E_C}\overline{\mathcal{M}^2} \tag{A.1}$$

In the rest frame of A [6]:

$$d\Gamma = \frac{|\vec{P}_c|}{E_A^2}\frac{d\Omega_C}{32\pi^2}\overline{\mathcal{M}^2} \tag{A.2}$$

The overlined matrix element $\overline{\mathcal{M}^2}$ implies averaging over spins:

$$\overline{\mathcal{M}^2} = \frac{1}{2}\sum_{spin}\mathcal{M}^\dagger\mathcal{M}$$

For the process $t \to ch$ the relevant part of the Yukawa Lagrangian (4.7) is

$$\mathcal{L}_{\overline{c}t} = -\frac{1}{\sqrt{2}}\overline{c}\rho_{ct}\cos(\beta-\alpha)t \equiv \overline{c}g_h t.$$

where $g_h = -\frac{1}{\sqrt{2}}\rho_{ct}\cos(\beta-\alpha)$ has been defined (for g_H simply change $-\cos(\beta-\alpha) \to \sin(\beta-\alpha)$ and $g_A = \frac{i}{\sqrt{2}}\rho_{ct}\gamma_5$). Assigning the four-momenta such that t has P_1, c has P_2 and h has P_3, the Feynman rules give that the matrix element $\mathcal{M}$ can be written as

$$\mathcal{M} = \overline{u}(P_2)(-ig)u(P_1)$$

$$\Rightarrow \mathcal{M}^\dagger\mathcal{M} = \overline{u}(P_1)(ig)u(P_2)\overline{u}(P_2)(-ig)u(P_1),$$

and

$$\begin{aligned}\overline{\mathcal{M}^2} = \frac{1}{2}\sum_{spin}\mathcal{M}^\dagger\mathcal{M} &= \frac{1}{2}g^2\mathrm{Tr}[(\not{P}_2 + m_c)(\not{P}_1 + m_t)] \\ &= \frac{1}{2}g^2\mathrm{Tr}[(\not{P}_2\not{P}_1 + m_c m_t)]\end{aligned} \tag{A.3}$$

Since P_1, P_2 are scalars in Dirac space (but not $\not{P}_2 = \gamma^\mu_{a,b}P_{2\mu}$ or $\not{P}_1 = \gamma^\nu_{b,c}P_{1\nu}$ since $\gamma^\mu_{a,b}$ and $\gamma^\nu_{b,c}$ have two Dirac indices and are matrices in Dirac space):

$$\mathrm{Tr}[\not{P}_2\not{P}_1] = \mathrm{Tr}[\gamma^\mu_{a,b}P_{2\mu}\gamma^\nu_{b,c}P_{1\nu}] = \mathrm{Tr}[\gamma^\mu_{a,b}\gamma^\nu_{b,c}]P_{2\mu}P_{1\nu} = 4g^{\mu\nu}P_{2\mu}P_{1\nu} = 4P_2^\mu \cdot P_{1\mu}.$$

The mass term in (A.3) is implicitly multiplied by a unity matrix, giving:

$$m_c m_t \mathrm{Tr}[1] = 4m_c m_t.$$

So

$$\overline{\mathcal{M}^2} = 2g^2(P_2^\mu \cdot P_{1\mu} + m_c m_t).$$

Putting this into the expression for the decay width in the rest frame of t (where $E_A = m_t$, $P_{1\mu} = (m_t, \vec{0})$ and $|\vec{P_c}| = |\vec{P_2}|$):

$$\begin{aligned} d\Gamma &= \frac{|\vec{P_2}|}{m_t^2}\frac{d\Omega_2}{32\pi^2}2g^2(P_2^\mu \cdot P_{1\mu} + m_c m_t), \\ &= \frac{|\vec{P_2}|}{m_t^2}\frac{d\Omega_2}{32\pi^2}2g^2(E_2 m_t + m_c m_t). \end{aligned}$$

Integrating over all angles possible (isotropic since no particular direction is preferred) and using that $E_2^2 = |\vec{P_2}|^2 + m_c^2$ gives

$$\Gamma = \frac{g^2}{4\pi m_t}|\vec{P_2}| \cdot \Big[\sqrt{|\vec{P_2}|^2 + m_c^2} + m_c\Big]. \tag{A.4}$$

For three-body scattering [19]:

$$\begin{aligned} |\vec{P_2}| &= \frac{m_t}{2}(1 + x_c^4 + x_h^4 - 2x_c^2 - 2x_h^2 - 2x_c^2x_h^2)^{\frac{1}{2}} = \frac{m_t}{2}\lambda^{\frac{1}{2}}(1, x_c^2, x_h^2) \\ &= \frac{m_t}{2}\sqrt{1-(x_h+x_c)^2}\sqrt{1-(x_h-x_c)^2}, \end{aligned} \tag{A.5}$$

where the kinematical factors are $x_c = m_c/m_t$ and $x_h = m_h/m_t$. $\lambda(1, x_c^2, x_h^2)$ is the Källén-function with proper arguments.

The factor $\Big[\sqrt{|\vec{P_2}|^2 + m_c^2} + m_c\Big]$ can be rewritten after some algebraic manipulation:

$$\begin{aligned} \Big[\sqrt{|\vec{P_2}|^2 + m_c^2} + m_c\Big] &= \Big[\frac{1}{2}(m_t^2\lambda(1, x_c^2, x_h^2) + 4x_c^2m_t^2)^{\frac{1}{2}} + x_c m_t\Big], \\ &= \frac{m_t}{2}\Big[(1 + x_c^4 + x_h^4 + 2x_c^2 - 2x_h^2 - 2x_c^2x_h^2)^{\frac{1}{2}} + 2x_c\Big], \\ &= \frac{m_t}{2}\Big[((1 + x_c^2 - x_h^2)^2)^{\frac{1}{2}} + 2x_c\Big] = \frac{m_t}{2}\Big[(x_c^2 + 2x_c + 1) - x_h^2\Big], \\ &= \frac{m_t}{2}\Big[(1 + x_c)^2 - x_h^2\Big]. \end{aligned} \tag{A.6}$$

So the decay width, using equations (A.5) and (A.6), is

$$\Gamma = \frac{g^2}{16\pi}m_t[(1 + x_c)^2 - x_h^2] \cdot \sqrt{1-(x_h+x_c)^2} \cdot \sqrt{1-(x_h-x_c)^2}. \tag{A.7}$$

For the CP-odd pseudoscalar A, because of the γ_5 matrix in the coupling g_A and since $\gamma_5 \not{P} = -\not{P}\gamma_5$, a minus sign appears in (A.3) that propagates to (A.7) and changes the plus in $(1 + x_c^2)$ to a minus, thus the expression in (4.15) is obtained.

□